Published on Transportation Research Part B: Methodological; DOI: 10.1016/j.trb.2026.103461; subject to CC BY-NC-ND license

A Three-sided Network Equilibrium Model for On-demand Food Delivery Services

Kaihang Zhang[a], Jintao Ke*[a], and Xiaolei Wang[b]

[a] *Department of Civil Engineering, The University of Hong Kong, Hong Kong, China*
[b] *School of Economics and Management, Tongji University, Shanghai, China*

Abstract

The on-demand food delivery (OFD) industry has experienced significant growth in recent years; however, this rapid expansion has also presented numerous operational challenges for OFD platforms. While existing studies on the operational design for OFD platforms offer valuable managerial insights, few of them have considered spatial heterogeneity which greatly impacts the OFD market because many drivers deliver orders as bundles, i.e., delivering multiple orders in a trip. This work develops a network equilibrium model to capture the complex interactions among the market's three major players, namely, customers, drivers, and merchants. We consider a game-theoretical framework in the Stackelberg leader-follower structure. As the leader, the OFD platform aims to achieve its desired objectives by leveraging two major operations: (1) the batch-matching between delivery drivers and orders, and (2) the bundling delivery dispatching which optimizes the drivers' routes in delivering multiple orders per ride. Three market players are regarded as followers, with their behaviors depicted by utility-based discrete choice models, and their interactions on a network scope captured by the three-sided network equilibrium model. We formulate the matching and delivering problem as a mathematical program with equilibrium constraints, and develop a coordinate descent–based algorithm to solve it efficiently. Through extensive numerical studies on real-world data, we showcase the efficacy of our proposed model in evaluating the performance of various operational strategies for OFD platforms. Our analysis offers insights into the impacts of platform operations on market players from a stationary equilibrium perspective. The proposed model can be utilized as an analytical tool to assist OFD platforms and the government in high-level planning that enhances efficiency and sustainability.

Keywords: On-demand food delivery; On-demand transport services; Network equilibrium; Bundling delivery; Mathematical programming with equilibrium constraints (MPEC).

*Corresponding author, email: kejintao@hku.hk

1 Introduction

In recent years, on-demand food delivery (OFD) services have experienced a remarkable surge, positioning it as one of the fastest-growing sectors in the service industry. According to The Business Research Company (2024), the online food delivery market is predicted to grow (at a compound annual growth rate) 11.5% from 2023 to 2024. This notable increase in popularity can be attributed to various socio-economic factors, including consumer preferences, advancements in digital technology, and post-COVID customer behavior, where, compared with dine-in in restaurants, many people have been used to reducing physical interactions and choose to order online. The OFD service offers several societal benefits, including convenient dining options for customers, flexible work opportunities for freelancers, and increased revenue for restaurants. These advantages have driven the growth of this type of service in recent years, and numerous large companies have emerged, including Uber Eats, DoorDash, and Deliveroo, among others.

However, there are also many challenges in OFD service design. In urban areas, people normally expect fast and high-quality delivery services, and they tend to prefer ordering food from anywhere and anytime, but in practice, the delivery drivers are not always available in the vicinity of their desired restaurants. This challenge requires the service provider to coordinate the delivery drivers wisely, even to reposition additional drivers from adjacent areas if necessary. Also, the complex interplay of customers, drivers, and merchants makes it more difficult to understand the market. For instance, market conditions, such as the customer demand, may impact whether a merchant is willing to be online to the OFD service and also impact the vacant drivers' cruising behaviors. Although the decision to join the OFD market can be long-term, it is also possible to be a short-term decision because some merchants have different schedules on the OFD platform. For example, be offline during peak hours and be online during off-peak hours. This paper emphasizes merchants' behavior on their within-day decision of whether to be online to the market and thus the number of merchants can be dynamic. Besides, the platform's operational strategies and commission/wage/fee schemes affect the system in a sophisticated way, especially in the vehicular flow of drivers in the urban road network. Therefore, understanding the operations of the OFD system and their effects on customers, drivers, and merchants is crucial, particularly when accounting for the spatial heterogeneity and network interactions that are prevalent within a transportation network.

The OFD service usually involves centralized operations from food delivery platforms and several market players (customers, drivers, and merchants), which is similar to other types of on-demand urban mobility services such as ride-sourcing (RS). However, compared with the RS service, there is an additional market player in the OFD service, namely, the merchant (or restaurant, we use these two terms interchangeably in this paper), other than the customers and delivery drivers. Merchants in the OFD market can decide whether they are online to the OFD platform or not, based on their perceived market conditions, which are influenced jointly by the behaviors of the other two players in the OFD market as well as the platform. On the other hand, the behavior of

the merchant, in turn, has an impact on others. The interplay among the three market players, therefore, brings more challenges to the operational management of the OFD service. On top of the additional market player, the frequent application of order bundling (also known as order consolidation) in OFD makes it more challenging than the operations in the RS market. The RS market, albeit there are also ride-sharing or pooling services, normally tackles the problem of delivering a single individual from one place to another. It is the nature of the RS service that does not allow it to deliver too many passengers in one route as it is majored at providing a timely mobility service. In contrast, it is more commonly seen in an OFD market that a driver picks up multiple orders and delivers them sequentially. The order assignment thus becomes more complex than that of the RS service due to order bundling. To this end, the OFD service appears to be more challenging than the RS service, and therefore, despite a rich body of literature in the RS community, the marked differences between RS and OFD markets makes it impractical to apply RS service models directly to the OFD service.

The OFD service is categorized into a type of transportation-enabled service within the transportation research community (Wang, 2022). The remarkable rate of growth exhibited by this phenomenon has captured considerable attention within the academic community, and many have raised concerns regarding the operational challenges (e.g., Li et al., 2020; Chen et al., 2022). However, existing works on analyzing the food delivery service design (e.g., Yildiz and Savelsbergh, 2019; Zhang et al., 2025) primarily concentrate on the system's overall performance from an aggregate level, but the detailed network-wide characteristics, such as the customer and driver flow on a transportation network, are not well studied. On the other hand, optimization-based models (e.g., Simoni and Winkenbach, 2023) primarily emphasize order assignment or routing problems, which are more suitable for real-time/short-term decision-making problems with a fixed set of customer requests and drivers. These optimization models do not usually capture the behaviors of customers, drivers, and merchants and their complex endogenous interactions. Thus, a network equilibrium model is needed to study how the three players respond to the OFD platform's operational strategies, as well as to analyze the managerial insights. By "managerial insights", we refer to the insights that is useful for managing an OFD market, which includes the market responses under different order dispatching strategies, the impact of bundling capacity, driver fleet size, and pricing strategies. These insights are helpful for platform operators or government practitioners to make decisions on the management of this market. This network model will be beneficial for OFD platforms in devising pricing, dispatching, delivery, and order bundling strategies while accounting for the behaviors of different players and network heterogeneity.

This paper develops a three-sided network equilibrium model of the OFD market. We design a mathematical framework to model the behaviors of the platform and three market players. A leader-follower game is adopted to depict the OFD system, where the platform acts as the leader and others are followers in response to the decisions from the platform. We consider two decision problems for the OFD platforms, namely the batch-matching problem and the bundling delivery

dispatching problem. In the batch-matching problem, the platform first accumulates a certain number of delivery drivers and order bundles and then pairs them up with a specific objective such as profit maximization. In the bundling delivery dispatching problem, order bundling is studied in this work which allows delivery drivers to carry more than one order in each delivery task. The platform determines optimal delivery sequences in each order bundling, aiming at minimizing either the wage cost for drivers or the customer waiting time. The proposed modeling framework provides analyses of the behaviors and resulting network flows of the three market players on a service network. We also study the pricing designs, including the commission extracted from merchants' revenue, the delivery fee collected from customers, and the wage paid by the platform to drivers. The main contributions of this work are summarized as follows.

1. We develop a three-sided network model to capture the behaviors and network flows of customers, drivers, and merchants in an OFD system. We consider the bundling delivery strategy as a dispatching problem by treating their movement with vehicular flows. This approach enables us to formulate bundling delivery into the joint optimization model of the OFD system and in an equilibrium state, termed the stationary matching and dispatching (SMD) problem.

2. Our model can capture the stationary matching between customers and drivers in a batch-matching procedure as well as the bundling delivery process. We formulate and compare three delivery strategies, namely the random-bundling strategy (RBS), the delivery cost minimization strategy (DCS), and the waiting time minimization strategy (WTS). We show our model's practical value in evaluating different operational goals and discuss the impacts of how different dispatching strategies to the system.

3. This study discovers the behaviors of network-wide interactions of the service network analysis with an additional market player, i.e., the merchant, compared with the two-sided ride-sourcing market and thus fills in the research gap. Considering the increased model complexity introduced by the new market player, we approximate the SMD problem using a coordinate descent–based iterative approach. Numerical experiments show that our approach is efficient while keeping good feasibility.

The rest of the paper is organized as follows. Section 2 summarizes the related work in the field of on-demand food delivery service and the network analysis in ride-sourcing service. Section 3 describes the convention used in this paper and a general framework of the problem. In Section 4, we first analyze the behaviors of three market players, and then state the three-sided network equilibrium conditions. We then present how we model the platform's decisions including batch-matching and delivery dispatching. Section 5 formulates the stationary matching and dispatching (SMD) decisions and the solution algorithm for the SMD problem. Section 6 demonstrates numerical experiments and Section 7 finally concludes the paper.

2 Literature review

A considerable number of research works have been done to design or understand the OFD services. We classify representative works into three categories. The first cluster of research investigates the empirical insights from real-world datasets or leverages the advantages of rich data availability and develops descriptive/data-driven methods. Mao et al. (2019, 2022) study the impact of early/late arrival of orders to the future customer behaviors as well as the impact of drivers' local geographical knowledge on the delivery time. Other research attempts to explore the insights from datasets/surveys and reveal practical values, such as Liu et al. (2023) who study the additional working opportunities for female workers thanks to the food delivery industry, Nguyen-Phuoc et al. (2022) who conduct a unique survey to study the traffic safety concerns due to OFD services, and Liang et al. (2024) who study the merchants' willingness to wait using a survival model. On the other hand, data-driven methods, especially machine learning techniques, appear to be popular in recent years. These efforts tackle the problems including the prediction on order information (e.g., Zhu et al., 2020; Liang et al., 2023), integration of prediction into operations (e.g., Hildebrandt and Ulmer, 2022), etc.

Besides the school of data-driven research, the second research stream concentrates on the operational optimization of vehicle routing or workforce scheduling. The OFD has been formulated into the meal delivery routing problem (Reyes et al., 2018), which is also considered as a variant of a more general cluster, the dynamic pickup and delivery problem (DPDP), such as Ulmer et al. (2021). We refer to Berbeglia et al. (2010) for a comprehensive review of DPDP. However, this type of problem is difficult to solve especially when considering integer programming, and various academic endeavors have been undertaken to develop effective solution algorithms for the optimization problem. Approaches such as heuristics (e.g., Simoni and Winkenbach, 2023), decomposition approaches (e.g., Ulmer et al., 2021), and machine-learning-based acceleration techniques (e.g., Behrendt et al., 2023) are of particular interest in the literature. In summary, these efforts are primarily focused on the operational strategies within the delivery service market which is more "microscopic". This involves developing solutions and techniques that optimize specific aspects of operations, such as route assignment, vehicle scheduling, and workforce scheduling, to improve overall efficiency and customer satisfaction, but the behaviors of customers, drivers, and merchants and their endogenous interactions remain unclear.

The third school of literature is the market equilibrium analysis of the OFD market which provides high-level managerial insights. These insights are of interest to decision-makers/system operators, especially for those who do not perform hands-on operations but need an overall understanding of the market, such as the government or the senior manager of a company. Existing studies predominantly concentrate on an aggregate level of analysis, adopting a "top-down" approach to study the system. These studies often employ logical reasoning and develop concise models to comprehend the behavior of market players within the delivery service market. By ex-

amining the market as a whole, these studies aim to gain insights into the "average" interactions of various stakeholders involved in the delivery service system. Yildiz and Savelsbergh (2019) are the first, to the best of the author's knowledge, to study the single-restaurant scenario and develop high-level insights regarding the size of the service region, probability of order acceptance, and platform profit. Ke et al. (2024) study the effect of order bundling and the delay due to food preparation time which was normally pre-assumed to be negligible by previous studies. Bahrami et al. (2023) proposed a modeling framework to study the three-sided market of the on-demand food delivery service which incorporates customers, drivers, and restaurants. Ye et al. (2024b) discovered the pricing and market equilibrium problem using a physical routing and matching model. Zhang et al. (2025) develop a model to analyze the impact of service region size and order bundling, and taking the food preparation time into consideration. To sum up, these aggregate models predominantly rely on strong assumptions that neglect the significance of spatial heterogeneity, both of which are crucial aspects of real-world operations. By simplifying spatial differences, such as using an a priori customer distribution, these models become susceptible to losing their practical values.

The OFD service exhibits various similarities with other urban mobility services such as the ride-sourcing (RS) service. In terms of time efficiency, both OFD and RS belong to demand-responsive service which is requested upon needed. Also, both services may rely on a centralized platform that organizes drivers to pick up passengers/meals and drop them off at pre-determined locations. In the context of RS research, numerous efforts have been made in the existing literature. They also span across the fields of aggregate analysis (e.g., Ke et al., 2020a; Yang et al., 2020), optimization and decision-making (e.g., Chen et al., 2020; Lyu et al., 2023; Courcoubetis et al., 2024), or network analysis (e.g., Yang and Wong, 1998; Yang et al., 2010; He and Shen, 2015; Xu et al., 2021). Notably, the ride-sharing (e.g., Wang et al., 2018; Di and Ban, 2019; Chen et al., 2025) and ride-pooling (e.g., Alonso-Mora et al., 2017; Ke et al., 2020b; Wang et al., 2021; Zhang and Nie, 2021; Bahrami et al., 2022) services are comparable to the OFD service because drivers also provide services to more than one customers. However, despite the similarity between RS and OFD, it is also discussed in the literature that human passengers are needier than packages (Daganzo and Ouyang, 2019), which underscores the differences between the OFD and RS service designing. Readers are directed to Wang and Yang (2019) for a comprehensive review of the literature in RS service.

Among the RS literature, those dealing with network analyses is of particular interest and most relevant to this study. Yang and Wong (1998) is the first study considering a network model to investigate the demand–supply relationship in the taxi market. They study the drivers' cruising behaviors in the road network and provide thorough analyses on the vehicle utilization, and drivers' waiting times. Yang et al. (2010) extend the network model and formally state the matching equilibrium (also termed the market clearing) in the taxi market and prove the existence of the equilibrium. The matching equilibrium differs from the traditional Wardrop user equilibrium (Wardrop, 1952) which is extensively studied by the transportation community. In user equilibrium, transportation

participants face alternative paths with the same utility and cannot benefit themselves by choosing any other options. However, in the matching equilibrium, the stationarity comes from the steady state of the matching rate (in the taxi market, it is the driver-passenger meeting rate) which makes the number of awaiting customers and vacant drivers in the system stable and invariant of time. In other words, new customer demands are constantly being generated but also matched with taxi drivers who are also ready to serve them, and finally, the system reaches a market clearing. Apart from the traditional taxi market, e-hailing using portable devices has become prevailing due to the development of smartphone technology. He and Shen (2015) develop a network equilibrium model for the e-haling of taxis. They conclude that the e-hailing mode can reduce the customer waiting time due to the small matching friction. Xu et al. (2021) develop a model including both market equilibrium and path equilibrium in the ride-sourcing context where many drivers are freelancing workers instead of dedicated taxi drivers. They extend the previous works by considering inter-regional matching instead of local matching strategy, and they propose a novel data-driven matching function inspired by circuit theory to obtain the matching rate between drivers and customers. In OFD, most recently, Ye et al. (2024a) develop a network-equilibrium model to answer questions of whether and if so, how can autonomous vehicle technology benefit the OFD market. However, the bundling strategy is restricted to those orders sharing similar origin-destination pairs. Besides, the merchant behavior is not fully studied.

The existing literature has contributed greatly to understanding and designing the OFD service, ranging from empirical analysis to optimization, and also aggregate analysis. However, few of them (only Ye et al., 2024a) consider the network equilibrium and the spatial heterogeneity is often over-simplified by aggregate analyses. In the RS research community, although many studies have investigated spatial heterogeneity and conducted follow-up equilibrium analysis, the operational strategy of the RS market cannot be directly applied to the OFD market because there are many differences between them. First, the ride-sourcing market involves two market players, namely customers and drivers, while the OFD market has three players: customers, drivers, and merchants (Bahrami et al., 2023). The analysis involving three market players brings many more challenges than that of a two-sided market. For instance, the traffic in the three-sided food delivery market will affect both merchants and customers, the interplay between which will in turn affect the drivers' behaviors. Second, the OFD service usually involves bundling delivery which allows each driver to carry more than one order in one delivery trip. The additional flexibility comes from the fact that inanimate objects (i.e., foods) are generally less needy than passengers. The bundling behavior makes the OFD market distinct from the ride-sourcing market because the delivery routing should be carefully designed otherwise significant detours would be generated. Current research attempt (Ye et al., 2024a) deals with the order bundling strategy using a simplified approach, i.e., only those with similar origin-destination pair can be bundled. However, this approach may lead to insufficient delivery supply within a local area and thus requires the platform to reposition additional drivers to supplement the delivery. Our model deals with order bundling

using an optimization model by treating the it as a dispatching problem. This process integrates the bundling delivery flow into the joint optimization, combining matching and dispatching,g and ultimately provides optimal solutions to decision makers. Overall, this paper develops equilibrium conditions that analyze the complex interplay among three market players under equilibrium. The network model considers the spatial demand imbalance and driver trip flow. We also contribute to the literature by developing a mathematical framework to describe and understand the platform operation (matching and dispatching) in a steady-state equilibrium scenario.

3 Problem definition

This section describes the network flow equilibrium problem in the OFD context. We study the stationary state of an OFD system considering the platform's batch-matching and the bundling delivery dispatching problems. These two decisions are not inclusive but contribute most to the behaviors of the other three stakeholders. Hence, the main emphasis of this paper diverges from the extensive existing literature on optimizing routing problems for either matching or delivery. Instead, it concentrates on the steady state of the system and explores the behaviors of various players and their endogenous interactions on a service network. The drivers' routing is focused on the path flow on each possible path under equilibrium. The glossary of notation is listed in Table 4 in Appendix A for easier access to the meaning of each symbol.

In the OFD market, we suppose there is a centralized platform and three market players: customers, drivers, and merchants. For drivers, each of them participating in the market can be one of the three statuses, namely "occupied" status (those are delivering meals to customers), "pickup" status (instantaneously after being matched), and "vacant" status (those are cruising to a waiting point or staying on standby for the next match). We consider an area (for example, a city) that consists of different regions, represented by nodes in a network ("region" and "node" are used interchangeably hereinafter). Let $(\mathcal{N},\mathcal{E})$ represent a network where $\mathcal{N}$ denotes the node set representing each region and $\mathcal{E}$ denotes the edge set representing the set of links between every two regions. Let $\mathcal{N}^{\text{cus}} \subseteq \mathcal{N}$ be the set of all the possible nodal locations of customers, $\mathcal{N}^{\text{mer}} \subseteq \mathcal{N}$ be the set of the nodal locations of merchants, and $\mathcal{N}^{\text{dr}} \subseteq \mathcal{N}$ be the set of all the possible waiting points for vacant drivers. A waiting point is a place where drivers may stay and wait for the next round of delivery tasks. Note that these three sets $\mathcal{N}^{\text{cus}}$, $\mathcal{N}^{\text{mer}}$, and $\mathcal{N}^{\text{dr}}$ are not necessarily mutually exclusive. Merchants are considered as clusters at each node to approximate the real-world situation that there is restaurant agglomeration. For instance, there are often food plazas in North America or a shopping mall in East Asia where many restaurants are located closely and OFD drivers can collect multiple orders from different restaurants from that cluster. We make an assumption, consistent with existing literature (e.g., Bahrami et al., 2023 and Zhang et al., 2025), that drivers collect a bundle of orders from a "restaurant cluster" before delivery.

In the OFD market, the platform operators need to manage a fleet of drivers to serve customers who are located at node $c \in \mathcal{N}^{\text{cus}}$ ordering meals from merchants at nodes $m \in \mathcal{N}^{\text{mer}}$. As discussed earlier in this section, two decisions are considered. The first decision is to coordinate matched drivers to pick up a bundle of meals from a merchant location, which is regarded as the *matching* problem to solve the matching flow, denoted λ^{μ}_{vm}, where the superscript μ stands for "matching" and the subscripts v and m stand for, from vacant drivers' waiting points at $v \in \mathcal{N}^{\text{dr}}$ to merchants' locations $m \in \mathcal{N}^{\text{mer}}$. We consider a batch-matching problem where some vacant drivers and some order bundles are first kept waiting at the matching pool and then paired after some time, aiming at improving the operation objective, such as platform profit. After matching, the matched drivers will pick up the orders and deliver them one by one at a flow λ^{μ}_{vm} which is a series of decision variables denoting the matching flow where the superscript represents "matching" and the subscripts stand for locational indexes.

The matched drivers may travel inter- or intra-regionally for pickup, based on the platform's matching decision. The intra-regional matching is most efficient if local drivers are sufficient to satisfy the delivery demand. The calculation of intra-regional distance is placed in Appendix B.1 where we borrowed the idea of catchment area of a merchant from existing literature, and keep the generality of the problem setting in this section. However, it is sometimes necessary to allocate drivers from other regions to pick up orders especially when local drivers are in short supply. This allocation of drivers is usually termed reposition in existing studies (e.g., Luo et al., 2023; Guan and Bao, 2024), and how to coordinate drivers from one region to another should be answered by solving a matching problem.

The second operational decision is to assign delivery drivers to the delivery routes to improve the efficiency of the bundling delivery. It is then termed the *bundling delivery dispatching* problem or the delivery dispatching problem for short. In each bundle, there could be orders from customers in different places. We define a bundle of customer orders as an *order bundle*, and the sequence to complete an order bundle is defined as the *delivery path*. We call the number of orders in a bundle the *bundling ratio* denoted k, and it should be satisfied that $k \leq \hat{k}$ where $\hat{k}$ is an exogenous variable representing the maximum allowable number of orders in a bundle, or the bundling capacity for short (restricted by safety considerations or physical capacity of vehicles). In the following, we use math language to formally define an order bundle.

Definition 1 (An order bundle of size k)**.** *Under a bundling capacity $\hat{k}$, for a bundling ratio $k \leq \hat{k}$, let B^k_m denote a possible order bundle of merchant at m, we say the bundle consists of a few orders $b_{m,j}$ indexed by j, i.e., $B^k_m := \{b_{m,j}\}$, where $b_{m,j} \in \mathcal{N}^{cus}$ are (repeatable) customer orders and $j = \{1, \ldots, k\}$.*

For any $k \leq \hat{k}$, the set of all possible bundles of size k of merchant at m is denoted as $\mathcal{B}^k_m := \{\text{all possible } B^k_m\}$. For all k, we denote all bundles (of all sizes) of merchants at m as $\mathcal{B}_m := \bigcup_k \mathcal{B}^k_m$. Here, we define an index set $\mathcal{I}_m$ containing all the indexes of $\mathcal{B}_m$, i.e., the i-th bundle in $\mathcal{B}_m$ is

written as $\mathcal{B}_{m,i}$ for $i \in \mathcal{I}_m$. Its cardinality $I_m := |\mathcal{I}_m|$ means the total number of possible order bundles from the merchant at m.

Definition 2 (Delivery path)**.** *Given $\mathcal{B}_{m,i}$, a delivery path $\mathcal{P}_{m,i}$ is defined as the shortest path starting from the merchant at m and visiting the customers in $\mathcal{B}_{m,i}$. The shortest-path length is denoted $d_{m,i}$.*

The calculation of the shortest-path distance requires the data of the distances between every two nodes of the network. In practice, we can pre-calculate all the distances of the inter-regional OD pairs (i.e., origin and destination are different) by algorithms such as Dijkstra's algorithm, and store them for calculating the distance of a delivery path.

In a stationary equilibrium, the flows of delivery paths remain consistent, with the equilibrium being contingent upon the platform's decision-making in matching and bundling dispatching problem. The delivery path flow, i.e., the vehicular flow of each delivery path, is denoted by $\lambda^o_{m,i}$, corresponding to a delivery path $\mathcal{P}_{m,i}$. The bundling delivery is one of the key differences between ride-sourcing and food delivery services. Because of order bundling, customers who arrive early may need to spend some additional waiting time for subsequent orders to form a complete bundle. Since bundling delivery requires delivery drivers to visit multiple customers, the visiting sequence becomes vital and differs from dispatching strategies. We compare three strategies in this paper for the bundling delivery dispatching problem, which are the random-bundling strategy (RBS) wherein the platform does not intervene in the delivery dispatching, the delivery cost minimization strategy (DCS) which emphasizes reducing the labor cost, and the waiting time minimization strategy (WTS) which aims to minimize the customers' total waiting time. The detailed formulation and discussion will be given later in Section 5.1.2.

Besides the platform's decision, three market players act in response to the platform operators' decisions. Customers decide whether and how to choose takeout food from which restaurant based on their perceived utility which is affected by the platform's decisions. Also, vacant drivers can freely travel across the network and choose the "best" (in terms of their perceived utility) waiting point where they will be matched to the next delivery task. Additionally, merchants decide whether to be online on the platform or not based on their perceived utility. Therefore, the food delivery system in a network context is a leader-follower game where the platform holds more superior information and makes decisions, while customers, drivers, and merchants are the followers. We examine the stationary state of the system, where there are three sides of interaction among the three players, thus we term it a *three-sided* equilibrium. At each time instant, the average number of awaiting (for matching) order bundles targeted at merchants at m, the average number of awaiting vacant drivers at v, and the average number of merchants that are willing to be online to the platform in the market at m, are denoted by m^{cus}_m, m^{dr}_v, and m^{mer}_m, respectively. The notational convention here is that the superscript denotes which entity (customer, vacant driver, or merchant) it represents, while the subscript denotes the locational index. To better understand the system,

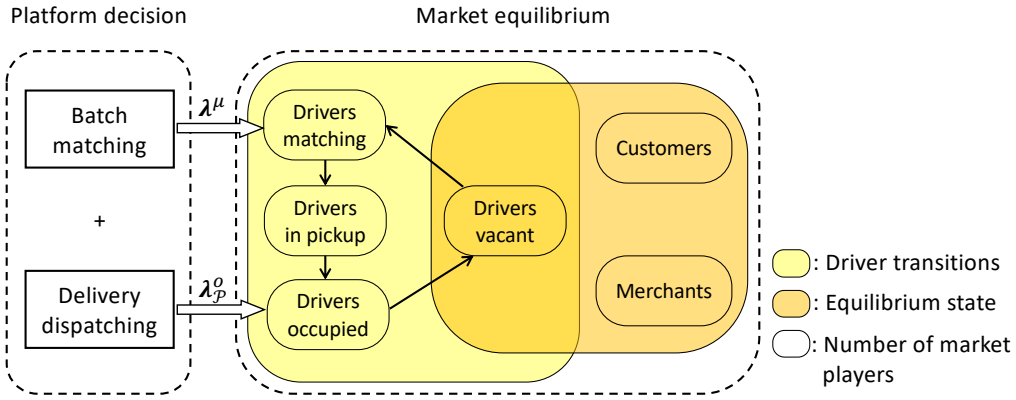

Figure 1: Diagram of the equilibrium of market players. The platform manipulates the market equilibrium through two decisions shown on the left. The market equilibrium is reflected by the number of market players (the orange block), and endogenously by driver status transitions (the yellow block).

we regard them as the *equilibrium variables* of the stationary state because their values contain information about the food delivery demand–supply relationship and merchant willingness to be online to the OFD market.

In summary, the platform performs the matching and delivery dispatching decisions, and in equilibrium, these decisions should be maintained at a stationary level. Let $\boldsymbol{\lambda}^{\mu}$ and $\boldsymbol{\lambda}^{o}_{\mathcal{P}}$ denote the vector form of batch-matching flow and delivery path flow, respectively, we need to solve them using the proposed modeling framework, depicted in Figure 1. Apart from the decisions, the defined three-sided market involves equilibrium problems, which makes the matching-dispatching problems become a mathematical program with equilibrium constraints (MPEC). The equilibrium variables m^{cus}_{m}, m^{dr}_{v}, and m^{mer}_{m} are solved by the equilibrium conditions (see formal definition in Section 4.2). We stack these equilibrium variables into a vector $\mathbf{m}$ for brevity. Then, we have $\mathbf{m} \in \mathcal{S}_e\left(\boldsymbol{\lambda}^{\mu}, \boldsymbol{\lambda}^{o}_{\mathcal{P}}\right)$ where $\mathcal{S}_e$ denotes the solution set of the equilibrium which is affected by the platform decisions $\boldsymbol{\lambda}^{\mu}$ and $\boldsymbol{\lambda}^{o}_{\mathcal{P}}$. With this setup, we name our problem as the stationary matching and dispatching (SMD) problem, and we formalize the stylized structure of SMD as illustrated in Figure 1 as follows:

$$
\begin{aligned}
[\text{SMD}] \quad \min_{\mathbf{m}, \boldsymbol{\lambda}^{\mu}, \boldsymbol{\lambda}^{o}_{\mathcal{P}}} \quad & f_{\mu}(\mathbf{m}, \boldsymbol{\lambda}^{\mu}) + f_{d}(\mathbf{m}, \boldsymbol{\lambda}^{o}_{\mathcal{P}}) && \text{(1a)} \\
\text{s.t.} \quad & \mathbf{m} \in \mathcal{S}_e\left(\boldsymbol{\lambda}^{\mu}, \boldsymbol{\lambda}^{o}_{\mathcal{P}}\right), && \text{(1b)} \\
& \boldsymbol{\lambda}^{\mu} \in \mathcal{F}_{\mu}(\mathbf{m}), && \text{(1c)} \\
& \boldsymbol{\lambda}^{o}_{\mathcal{P}} \in \mathcal{F}_{d}(\mathbf{m}, \boldsymbol{\lambda}^{\mu}), && \text{(1d)}
\end{aligned}
$$

where $f_{\mu}(\cdot)$ and $f_{d}(\cdot)$ represent the batch-matching and delivery dispatching objectives, respectively. The customer demand and the vacant driver flow are two intermediate variables in the equilibrium condition. The symbol $\mathcal{F}_{\mu}$ in Equation (1c) denotes the feasible set of the matching flow which will be defined in Section 5.1.1, and $\mathcal{F}_{d}$ in Equation (1d) denotes the feasible set of the delivery path

flow defined later in Section 4.2. The equilibrium conditions Equation (1b) makes the problem belong to the category of MPEC. In the following two sections, we first formulate the customers', drivers', and merchants' behaviors, followed by a formal definition of the three-sided equilibrium conditions, and then characterize the platform's decisions.

4 The three-sided equilibrium

This section presents the network equilibrium model for the three-sided OFD market. The OFD market serves customers at the demand rate of q. The demand rate varies across each OD pair in the network and it is dependent on both the customers' location and the interplay with merchants/drivers. The drivers in three statuses are traveling in the network and their vehicular flow from one region to another is denoted by $\boldsymbol{\lambda}^o$ for occupied drivers, $\boldsymbol{\lambda}^\varphi$ for vacant drivers, and $\boldsymbol{\lambda}^p$ for pickup drivers. We should assume a frictionless process when a driver receives a matching decision which yields $\boldsymbol{\lambda}^p = \boldsymbol{\lambda}^\mu$. In this section, we first formulate the demand and supply of the OFD service based on each market player's choice behaviors and then analyze the equilibrium conditions and properties.

4.1 Customers, vacant drivers, and merchants as followers

As briefly introduced in Section 3, customers, vacant drivers, and merchants interact in response to the decisions made by the platform, thus, we treat them as followers in the market. These three entities make decisions about whether and how to join the market based on their perceived utilities. As a result, m_m^{cus}, m_v^{dr}, and m_m^{mer} reflect the equilibrium state of the three-sided equilibrium, and mathematically, they are three sources of the degrees of freedom of the system.

4.1.1 Behavior of customers

We consider the random utility model to capture customer demand following the archetypes of existing literature (Ben-Akiva and Lerman, 1985; He and Shen, 2015; Xu et al., 2021). A customer at node $c \in \mathcal{N}^{\text{cus}}$ selects a merchant at $m \in \mathcal{N}^{\text{mer}}$ depending on their perceived utility, and the perceived utility is directly impacted by the platform's service quality. Two representative waiting times, namely the average matching time and delivery time, reflect the service quality of an OFD platform. These two types of waiting times are commonly displayed to customers via the OFD mobile APPs, thus we assume they are known a priori to customers before they make order requests. Later in Section 5.1.2, we discuss in detail about four types of waiting times that majorly impact the service quality, including matching, pickup, delivery, and order accumulation time. Yet in this section, we mainly discuss the matching and delivery times that directly impact customers' demand while leaving the other two to be specified later. We consider four factors governing the customers'

utility, (1) the attractiveness of merchants in region m to customers in region c, denoted by $A^{\text{cus}}_{c,m}$, (2) the delivery fee, which is the product of the delivery fee per distance p (\$/km) and the distance from the customer at c to the desired merchant at m, denoted by L_{cm}, (3) the average matching time W^{cus}_m of selecting merchants at m, and (4) the average delivery time as a function of delivery path flow, i.e., $W^{cd}_{c,m} = W^{cd}_{c,m}(\boldsymbol{\lambda}^o_{\mathcal{P}})$ for customer at c ordering food from merchant at m where the superscript stands for "customer delivery time" and subscript stands for locational indexes. Let β (\$/hour) be the value of time, the random utility (in the unit of \$) of a customer in region c selecting the merchant at m is given by

$$U^{\text{cus}}_{c,m} = V^{\text{cus}}_{c,m} + \varepsilon = A^{\text{cus}}_{c,m} - \theta^{\text{cus}} \cdot \left[pL_{cm} + \beta W^{\text{cus}}_m + \beta W^{cd}_{c,m} \right] + \varepsilon, \tag{2}$$

where ε is the perception error that follows the Gumbel distribution (a standard assumption in discrete choice theory, yielding logit-like formula, see Train, 2009, pp41–85). In the following, we discuss in detail the attractiveness, matching time, and delivery time in Equation (2).

Attractiveness to customers. The attractiveness term captures how desirable for a customer to order food from a target node, and we assume that the attractiveness is only dependent on the targeting node, not on its adjacent nodes. We consider that the attractiveness of merchants to customers in each region $A^{\text{cus}}_{c,m}$ is an increasing function of the number of merchants in that region. This assumption aligns with the study in economics. Konishi (2005) argue that "higher concentration of stores may attract more customers" even under choice uncertainty. Leonardi and Moretti (2023) argue that those areas with higher numbers of restaurants may attract more demand because of the agglomeration effect. The specific form can be empirically calibrated by practitioners, and in this study we adopt a relationship with decreasing marginal utility gain from an increasing number of merchants, see our discussion in Appendix B.2.

Matching time. We define the matching time at merchant node m as the expected time an order bundle spends in the "awaiting-assignment" state before a driver is dispatched to pick it up. Following Little's law Little, 1961, this quantity is obtained by dividing the steady-state quantity in the matching queue by the corresponding assignment throughput (matching flow). In our notation, m^{cus}_m denotes the number of customer order bundles waiting at merchant m, and λ^{μ}_{vm} is the assignment flow from drivers located at node v to merchant m (so $\sum_v \lambda^{\mu}_{vm}$ is the total rate at which orders in m served by drivers). Under the standard stationarity and rate-stability conditions (arrivals into the matching state equal departures via assignment), the matching time is

$$W^{\text{cus}}_m = \frac{m^{\text{cus}}_m}{\sum_v \lambda^{\mu}_{vm}}. \tag{3}$$

Delivery time. Each customer in a bundle experiences different delivery times. Suppose the customer demand from each customer location c to any desired merchant at m is known, denoted in the vector form $\mathbf{q}$, and given $\boldsymbol{\lambda}^o_{\mathcal{P}}$, we can use a linear transformation to compute the average customer delivery time $W^{cd}_{c,m}$.

Claim 1. *Given* $\mathbf{q}$, $W^{cd}_{c,m}$ *and* W^{cd} *can be obtained by linear transformations from* $\boldsymbol{\lambda}^o_{\mathcal{P}}$.

Proof. See proof in Appendix C. □

We notice that we need to obtain the customer demand $\mathbf{q}$ before computing $W^{cd}_{c,m}$, but we calculate $W^{cd}_{c,m}$ is for computing $\mathbf{q}$. Therefore, obtaining customer demand is a fixed-point system which we formulate in Section 4.2.

Customer demand flow With the utility function in Equation (2), we are ready to formulate the food delivery demand of a customer at c choosing to order from a merchant at m (or not using the food delivery platform), denoted as $q_{c,m}$ as an element of the vector $\mathbf{q}$. Suppose the total demand initiated from customers in the region c is known, and under Gumbel error in customers' utility perception, the demand rate is

$$q_{c,m} = \hat{q}_c \frac{\exp\left(V^{\text{cus}}_{c,m}\right)}{\exp\left(V^{\text{cus}}_0\right) + \sum_{m' \in \mathcal{N}^{\text{mer}}} \exp\left(V^{\text{cus}}_{c,m'}\right)}, \tag{4}$$

where V^{cus}_0 denotes the utility of choosing other dining options apart from the food delivery service, such as cooking or visiting restaurants in person. According to Equation (4), if customers' utility of choosing a merchant decreases, the demand rate will also decrease and these demands will go to other means of dining. Since distance is a relatively deterministic factor, the matching time and the delivery time in a region play a pivotal role in attracting customers from other means of dining to use the food delivery service. Thus, an effective matching and dispatching strategy becomes crucial.

4.1.2 Behavior of vacant drivers

Drivers are followers in the market in two aspects. First, we consider an elastic vehicle fleet, which means the fleet size is down to the choice of drivers who are usually freelancers in food delivery services (Sun et al., 2019; Wang, 2022). This type of worker typically designs their own schedules based on their perceived utility of joining the market. In this study, we simplify the relationship of the fleet size by assuming an increasing function of the average earning $\bar{F}$ which will be discussed in detail in Section 4.2. This section focuses on the movement of vacant drivers and the corresponding vehicular flow.

Apart from the total vehicle supply, the movement of vacant drivers is also decided by the vacant drivers themselves. Vacant drivers make decisions based on their perception which is influenced by the platform's decisions and the behavior of other market players. A food delivery driver will become vacant status after the completion of delivering all the orders from the previous bundle. These vacant drivers will decide where to go among a set of potential waiting points that are within the matching area of at least one of the merchants. We use random utility theory to capture the movement of vacant drivers as well. Assume that an occupied driver completes their delivery at a customer's location $c \in \mathcal{N}^{\text{cus}}$. This driver decides to go to the next waiting point at $v \in \mathcal{N}^{\text{dr}}$ (which is within a matching area $\mathcal{N}_m^{\text{match}}$ of a merchant) based on the total utility of this movement. From the literature (Xu et al., 2021), the total utility of vacant drivers, denoted by U_{cv}^{dr}, is composed of two aspects. First, the expected earnings, and second, the expected time cost if traveling to node v:

$$U_{cv}^{\text{dr}} = V_{cv}^{\text{dr}} + \varepsilon = A_{cv}^{\text{dr}} + \theta^{\text{dr}} \left[\check{F}_v - \beta \left(\check{h}_v + h_{cv} + W_v^{\text{dr}} \right) \right] + \varepsilon, \tag{5}$$

where $\check{F}_v$ is the expected earning rate if traveling to node v, $\check{h}_v$ is the expected service time if traveling to node v, h_{cv} is the travel time from c to v. Similar to the customers, W_v^{dr} is the average matching time if waiting at node v where $W_v^{\text{dr}} = m_v^{\text{dr}} / \sum_m \lambda_{vm}^{\mu}$, computed from using Little's formula. The perception error ε follows the Gumbel distribution to derive the logit-based choice model (Train, 2009). Similar to the way we describe the customers' preferences, we consider that vacant drivers' choices are also influenced by the attractiveness of each region A_{cv}^{dr} to vacant drivers. We make a mild assumption that the attractiveness of a region to drivers is positively related to the number of merchants in that region because more restaurants mean more working opportunities, see detailed discussion in Appendix B.3. The expected earnings at node v is the expectation of the average earnings of drivers serving merchants at m, weighted by the flow-based probability. Let $\bar{F}_m$ denote the average earning of the driver serving the merchants at node m, the average earning for vacant drivers moving to node v is

$$\check{F}_v = \frac{\sum_m \lambda_{vm}^{\mu} \bar{F}_m}{\sum_m \lambda_{vm}^{\mu}}, \tag{6}$$

where λ_{vm}^{μ} is the matching flow from node v to a merchant at node m for order pickup. The average earning rate of a driver serving merchants at m is

$$\bar{F}_m = \frac{\sum_{i \in \mathcal{I}_m} \lambda_{m,i}^{o} [w_0 + w d_{m,i}]}{\sum_{i \in \mathcal{I}_m} \lambda_{m,i}^{o}}, \tag{7}$$

where we consider the wage policy is based on the per-km wage w multiplied by distance plus a minimum wage w_0, and $d_{m,i}$ is the shortest-path distance following the path $\mathcal{P}_{m,i}$.

The expected time cost is related to the length of service time, which consists of two parts, the

pickup time and the delivery time. It is the expectation of the average service time for matching to merchants at m, weighted by the flow. Let $\bar{h}_m$ denote the average delivery time of the driver serving the merchants at node m, the expected time cost for traveling to node v is

$$\check{h}_v = \frac{\sum_m \lambda^{\mu}_{vm}(h_{vm} + \bar{h}_m)}{\sum_m \lambda^{\mu}_{vm}}, \tag{8}$$

where the average delivery time for drivers serving the merchants at node m is

$$\bar{h}_m = \frac{\sum_{i \in \mathcal{I}_m} \lambda^{o}_{m,i} \left[\frac{d_{m,i}}{v} + kt_s\right]}{\sum_{i \in \mathcal{I}_m} \lambda^{o}_{m,i}}, \tag{9}$$

where t_s denotes the dwell time for completing each delivery of an order. Then, the OD flow of vacant drivers is calculated using the logit-based choice model as

$$\lambda^{\varphi}_{cv} = \frac{\exp\left(V^{\mathrm{dr}}_{cv}\right)}{\sum_v \exp\left(V^{\mathrm{dr}}_{cv}\right)} \lambda_c, \tag{10}$$

where λ_c represents the inflow of the occupied drivers who have their last order (in the bundle of k orders) at c and it is computed by

$$\lambda_c = \sum_m \sum_{\substack{i \text{ that } \mathcal{P}_{m,i} \\ \text{ended at } c}} \lambda^{o}_{m,i}. \tag{11}$$

Claim 2. *Equation (11) can be written in vector form as*

$$\boldsymbol{\lambda}_c = \mathbf{M}^{ce} \boldsymbol{\lambda}^{o}_{\mathcal{P}}. \tag{12}$$

Proof. See Appendix D. □

In practice, this vectorization process exogenizes the condition sentence in Equation (11) and can significantly accelerate the computing speed.

4.1.3 Behavior of merchants

Merchants in region $m \in \mathcal{N}^{\mathrm{mer}}$ decide whether to be online on the OFD platform or not depending on their perceived utility of using the online food delivery platform. With a known total number of restaurants in the region m as $\hat{m}^{\mathrm{mer}}_m$, the actual number of restaurants willing to be online to the platform can be approximated by $\hat{m}^{\mathrm{mer}}_m$ multiplied by a proportion obtained from a logit-based choice model. Existing studies have argued the importance of delivery drivers to the merchants' decision on joining the market (Du et al., 2023). Also, Hu et al. (2024) argue that online sales

benefit from concentrated delivery drivers in the city center. Thus, we first assume that the more vacant drivers awaiting in that region, the more restaurants will be willing to be online to the OFD platform because a sufficient number of vacant drivers can provide a guarantee of delivery efficiency and service quality. Second, we consider the dependency of customer demand. Since the platform charges the merchant a certain amount of commission for using the delivery platform, which we assume is linearly dependent on the price of each order, the impact of demand to merchants' utility is not monotone, i.e., it is positive under a low commission rate while negative under a large commission rate. Then, the merchants' utility is formulated as

$$U_m^{\mathrm{mer}} = V_m^{\mathrm{mer}} + \varepsilon = \theta_1^m m_m^{\mathrm{dr}} - \theta_2^m \gamma p_o \sum_c q_{c,m} + \theta_0^m + \varepsilon, \tag{13}$$

where m_m^{dr} denotes the number of awaiting vacant drivers (superscript) at region m (subscript), γ the proportion of revenue charged by the platform, p_o the average price of each order, and $\theta_i^m, i \in \{1,2\}$ the coefficients of number of vacant drivers nearby and commission, respectively; and θ_0^m the intercept that captures unobserved factors that contributes to the utility. Notably, the quantity m_m^{dr} is not exogenous local counts but the endogenous equilibrium variables obtained from system-wide flow balance, vehicle conservation, and fixed-point constraints. Consequently, the numbers of vacant drivers and merchant that are willing to join the market are already functions of the entire network state (including nodes within the matching distance), so utilities written as $U_m^{\mathrm{mer}}\left(\cdot, m_m^{\mathrm{dr}}\right)$ are reduced-form summaries of broader neighborhood availability. Then, the number of merchants at region m that are willing to be online to the platform is given by

$$m_m^{\mathrm{mer}} = \frac{\exp\left(V_m^{\mathrm{mer}}\right)}{1+\exp\left(V_m^{\mathrm{mer}}\right)} \hat{m}_m^{\mathrm{mer}}. \tag{14}$$

The number of merchants in a region influences both customers and vacant drivers. If the number of merchants in a region increases, the level of attractiveness of a region to customers will increase because there are more dining options. It also increases the vacant drivers' utility because more restaurants mean more potential customer demand and thus a higher probability of being matched to a delivery task. However, either the awaiting vacant drivers or order bundles cannot exceed a limit because too many of them accumulated at the merchants' places will generate substantial matching time and ultimately reduce their utility. These two opposite driven forces will finally achieve a balance among the three market players in the system where the system tends to be steady.

4.2 Equilibrium conditions

The three-sided equilibrium describes the long-term stationarity of the system. The equilibrium conditions include the demand–supply balance, the fixed-point constraint for customer demand

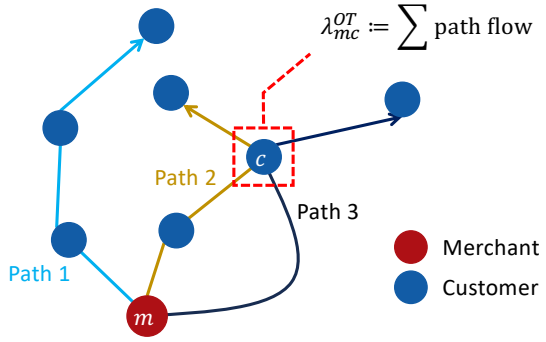

Figure 2: Delivery path flows and the flux through each customer location.

generation, flow balance, and vehicle fleet reservation. With a slight abuse of notation and to maintain neatness, we do not include the randomness in the customer demand and vacant driver flows (on their attractiveness) until the solution section. Our approach on dealing with the randomness in the constraints also follow the structure in Boyd and Vandenberghe (2004, pp. 209), namely considering the expected scenarios for constraints.

If we define the term "delivery supply" to describe the ability of delivering food by the realized fleet, we have the first condition, namely the food delivery supply should meet the customer demand rate. The food delivery supply here is considered as the origin-throughput (OT) trip flow rather than the origin-destination (OD) trip flow in the conventional ride-sourcing market because of the bundling delivery. In delivery with bundling, a delivery path can serve multiple customers at different nodes along its route; hence the delivery supply at a node is determined by whether an occupied driver visits that node, not solely by their terminal destination. We therefore define the origin-throughput (OT) flow at node v as the aggregate rate of occupied delivery paths that traverse v (including if v is the final stop). In other words, every delivery driver traveling through a location would contribute to the delivery supply to that region. When each tour serves exactly one destination, OT reduces to the usual OD flow; with bundling, OT generalizes OD by crediting each visit with one unit of service at the visited node. The OT flow is obtained by computing the trip flux of each region, i.e., the summation of delivery path flow going through each region, see Figure 2 as a depiction. The delivery demand–supply equilibrium is expressed as

$$\lambda_{mc}^{OT} = \sum_{\substack{i \text{ that } \mathcal{P}_{m,i} \\ \text{through } c}} \lambda_{m,i}^{o} = q_{c,m}. \tag{15}$$

As we do in Claim 2, to accelerate the computing, we can remove the condition sentence in Equation (15) by constructing the vectorized form of the food delivery supply using an exogenous matrix $\mathbf{A}$ with a dimension of $|c| \cdot |m|$ by $|\boldsymbol{\lambda}_{\mathcal{P}}^{o}|$. This matrix transforms the delivery path flow to the delivery supply rate, i.e., mapping from $\boldsymbol{\lambda}_{\mathcal{P}}^{o}$ to $\boldsymbol{\lambda}^{o}$, and the constraint requires $\boldsymbol{\lambda}^{o} = \mathbf{q}$. Thus,

we can have the following

Claim 3. *Equation (15) can be written to vector form as*

$$\boldsymbol{\lambda}^o = \mathbf{A}\boldsymbol{\lambda}^o_{\mathcal{P}} = \mathbf{q}. \tag{16}$$

Proof. See Appendix E. □

Second, the customer demand should be solved from a fixed-point system, because demand is dependent on delivery time while delivery time is in turn dependent on demand. Using a general form, Equations (2) and (4) can be written as

$$\mathbf{q} = g(\mathbf{m}, \boldsymbol{\lambda}^\mu, \boldsymbol{\lambda}^o_{\mathcal{P}}), \tag{17}$$

representing the customer demand generation process. On the other hand, suppose a healthy market condition, under a given demand $\mathbf{q}$, there is always an operational decision $\boldsymbol{\lambda}^o_{\mathcal{P}}$. Therefore, with a slight abuse of notation, we can treat $\boldsymbol{\lambda}^o_{\mathcal{P}}$ as a general function of $\mathbf{q}$, i.e., $\boldsymbol{\lambda}^o_{\mathcal{P}} = h(\mathbf{q})$ although the mapping from $\mathbf{q}$ to $\boldsymbol{\lambda}^o_{\mathcal{P}}$ is an optimization problem under some operational objectives (see DCS and WTS in Section 5.1.2). Then, we have the following fixed-point problem as a constraint for the equilibrium.

$$\mathbf{q} = g(\mathbf{m}, \boldsymbol{\lambda}^\mu, h(\mathbf{q})). \tag{18}$$

Third, the matching and dispatching of food delivery drivers should maintain stationarity, namely the matching rate equaling the rate of drivers becoming vacant (and also ready for matching), and the rate of dispatched drivers (equals matching rate) for delivery equaling to the rate of drivers becoming occupied. These two conditions are formulated by Equations (19) and (20) as follows, respectively:

$$\sum_m \lambda^\mu_{vm} = \sum_c \lambda^\varphi_{cv}(\mathbf{m}, \boldsymbol{\lambda}^\mu, \boldsymbol{\lambda}^o_{\mathcal{P}}), \tag{19}$$

$$\sum_{v \in \mathcal{N}^{\text{match}}_m} \lambda^\mu_{vm} = \sum_{i \in \mathcal{I}_m} \lambda^o_{m,i}, \tag{20}$$

where $\mathcal{N}^{\text{match}}_m$ represents the matching area of merchants at m. Also, the rate of drivers moving from the occupied status to the vacant status should also be equal:

$$\sum_m \sum_{\substack{i \text{ that } \mathcal{P}_{m,i} \\ \text{ended at } c}} \lambda^o_{m,i} = \sum_v \lambda^\varphi_{cv}(\mathbf{m}, \boldsymbol{\lambda}^\mu, \boldsymbol{\lambda}^o_{\mathcal{P}}), \tag{21}$$

which is an already-satisfied condition in this study because the vacant drivers flows are computed

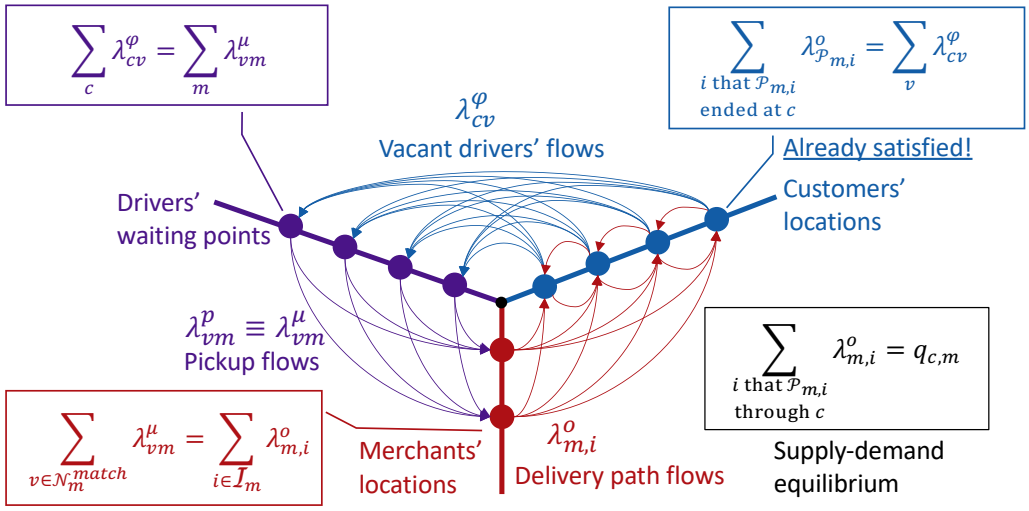

Figure 3: The three-sided food delivery flow conservation and demand–supply equilibrium.

using the behavior choice model (see Equations (10) and (11) in Section 4.1.2 for details). Therefore, Equation (21) becomes redundant constraints and can be removed without affecting the system.

Equations (19) to (21) establish the three-sided flow equilibrium of matching and dispatching in an on-demand food delivery system, as depicted in Figure 3. It differs from the two-sided network equilibrium of the ride-sourcing market (Xu et al., 2021) by the presence of the additional player (the merchants) which makes it more complex for modeling order consolidation and route assignment in a network equilibrium model. The different delivery destinations are generally difficult to achieve in the ride-pooling services because it is hard to ask passengers to gather at a meeting point while it is easier to achieve in the food delivery market. Apart from the difference between the ride-sourcing and the food delivery markets, our network equilibrium also exhibits advantages over the aggregate equilibrium models, such as that of Bahrami et al. (2023). The network equilibrium captures spatial heterogeneity better than the aggregate models by its nature, by locational-specific choice–based flows. The network models are also beneficial for practitioners to design and implement operating strategies on real transportation networks.

Due to the friction of matching and dispatching, it is easy to understand that there will be a certain number of awaiting drivers and awaiting order bundles accumulated in the market. Also, since not all merchants are willing to be online on the platform, the number of merchants willing to be online will be less than the total (exogenous) number of merchants, but ultimately tends to achieve a steady state. These three groups of variables can be treated as the equilibrium variables of the stationary state as we discussed earlier in Section 3. We have equilibrium variables m_v^{dr}, m_m^{cus}, and m_m^{mer} so there are $v+2m$ unknown variables (the customer demand rate can be obtained by the fixed-point system so the number of equations and the number of unknown variables cancel out). On the other hand, in terms of the number of equations, there are $v+m$ valid equations

in Equations (19) and (20), and from Section 4.1.3 there are m additional equations for obtaining m_m^{mer}, which lead to a total of $v+2m$ equations established. However, Equations (19) to (21) form a closed loop, which means that there must be one redundant degree of freedom. As a result, the number of valid equations is $v+2m-1$ which is less than the number of the system's equilibrium variables. The missing equation elicits the vehicle conservation condition which restricts the total number of food delivery drivers:

$$\underbrace{\hat{N}_F \cdot f(\bar{F})}_{=:N_F} \equiv \sum_m \sum_{i\in\mathcal{I}_m} h_{m,i}\lambda^o_{m,i} + \sum_c \sum_v h_{cv}\lambda^{\varphi}_{cv}(\mathbf{m},\boldsymbol{\lambda}^{\mu},\boldsymbol{\lambda}^o_{\mathcal{P}}) + \sum_m \sum_v h_{vm}\lambda^{\mu}_{vm} + \sum_v m_v^{\text{dr}}, \tag{22}$$

where $\hat{N}_F$ is an exogenous variable meaning the total number of freelancing delivery drivers that may enter the market for delivery work (total fleet, exogenous); N_F denotes the realized number of delivery drivers in the market in the equilibrium state (realized fleet); $h_{m,i} := d_{m,i}/v$ means the travel time of path $\mathcal{P}_{m,i}$; and h_{xy} means the travel time from x to y. This process allows us to consider the elastic delivery labor supply, which is endogenously determined in the market equilibrium (Angrist et al., 2021). We shall make a mild assumption that the realized number of delivery drivers is positively related to the average earning $\bar{F}$ (see the labor supply study of freelancing drivers by Sun et al., 2019), which means $\partial f/\partial \bar{F} > 0$. In this work, we allow the vehicle fleet size as well as all the equilibrium variables to be decimal numbers for approximation because our modeling framework aims at describing the system by looking at a stationary equilibrium.

Thus far, we have established the demand–supply equilibrium and the three-sided matching-dispatching network equilibrium conditions. We are now ready to formally state the three-sided network equilibrium of the OFD system as follows.

Definition 3 (Three-sided network equilibrium)**.** *For any decision variables $\boldsymbol{\lambda}^{\mu}$ and $\boldsymbol{\lambda}^o_{\mathcal{P}}$, the on-demand food delivery service is said to achieve a stationary equilibrium if the equilibrium variable* $\mathbf{m}$ *satisfies the following equilibrium conditions are satisfied:*

$$\begin{cases} \mathbf{A}\boldsymbol{\lambda}^o_{\mathcal{P}} = \mathbf{q}, \\ \mathbf{q} = g(\mathbf{m},\boldsymbol{\lambda}^{\mu}, h(\mathbf{q})), \\ \sum_m \lambda^{\mu}_{vm} = \sum_c \lambda^{\varphi}_{cv}(\mathbf{m},\boldsymbol{\lambda}^{\mu},\boldsymbol{\lambda}^o_{\mathcal{P}}), \\ \sum_{v\in\mathcal{N}_m^{match}} \lambda^{\mu}_{vm} = \sum_{i\in\mathcal{I}_m} \lambda^o_{m,i}, \\ N_F = \sum_m \sum_{i\in\mathcal{I}_m} h_{m,i}\lambda^o_{m,i} + \sum_c \sum_v h_{cv}\lambda^{\varphi}_{cv}(\mathbf{m},\boldsymbol{\lambda}^{\mu},\boldsymbol{\lambda}^o_{\mathcal{P}}) + \sum_m \sum_v h_{vm}\lambda^{\mu}_{vm} + \sum_v m_v^{dr}. \end{cases} \tag{23}$$

It is also said that the market is clearing. During equilibrium, the number of awaiting order bundles, vacant drivers, and merchants in the market remains the same for every matching interval.

Among these flows, the batch-matching flow and the delivery path flow are obtained by solving the SMD in Equation (1), while the vacant drivers' flow and the customers' demand rate are computed by a closed-form formula using the logit-based choice model, see Section 4.1 for detailed analysis. The existence of the equilibrium is stated as follows (see proof in Appendix F). Again, as we discussed in Section 2, the equilibrium here in the network model is different from the user equilibrium by Wardrop (1952), which is a steady state regarding the users' travel preference when facing different route choices. Our equilibrium, also the matching equilibrium of taxi, e-hailing, and ride-hailing markets (Yang et al., 2010; He and Shen, 2015; Xu et al., 2021), comes from the consecutive matchings performed by the platform, resulting in a stationary state for the equilibrium variable $\mathbf{m}$, meaning that the number of awaiting order bundles, vacant drivers, and remaining merchants are stationary in the system.

Proposition 1 (Existence of equilibrium)**.** *There exists a three-sided equilibrium satisfying the equilibrium condition as described in Definition 3.*

Proof. See Section F. □

5 The stationary matching and dispatching

This section discusses the two decisions we considered from the platform's side, namely the matching and delivery dispatching decisions. Also, with the mathematical formulation, we develop a solution algorithm to solve the stationary matching and dispatching (SMD) problem. We focus more on the planning value of our model. Therefore, the problem solves the continuous customer demand rate and vehicular flow instead of focusing on solving vehicle routing problems which are typically integer programming problems. For readability, we discuss the objective of the SMD problem using two subsections. Although they should be considered as a whole in the SMD (see Figure 1), considering the computational efficiency, we discuss later in Section 5.3 that we approximate the SMD problem with a two-stage iterative algorithm which is particularly beneficial when dealing with larger-scale networks in practice.

The first decision problem is matching. We consider a batch-matching process, in which the platform dwells for a certain duration to accumulate some drivers and order bundles and then perform matching altogether. The second decision problem is dispatching. We consider bundling delivery, which allows multiple orders in each delivery route. We compare three different delivery dispatching strategies based on the different goals of operation from the platform, which are, the random-bundling strategy (RBS), the delivery cost minimization strategy (DCS), and the waiting time minimization strategy (WTS).

5.1 Platform's decisions on matching and delivery dispatching

The food delivery platform coordinates the drivers to serve the delivery demands of customers. This section describes the platform's decision-making processes as a leader to achieve certain objectives in batch-matching and delivery dispatching problems.

We discuss three assumptions before we delve into the details of the platform's decision. First, we assume that the uncertainty regarding delivery drivers' attitudes toward the pickup advisory is negligible, where the pickup advisory provides the suggested pickup destinations (merchant places) based on the batch-matching results. In practice, there will be some drivers who do not follow the pickup routing advisory (see Li and Phillips, 2018 and Liu et al., 2021) such that the efficiency of the batch-matching process is reduced. In this study, we focus on formulating the SMD problem but do not consider this uncertainty. Secondly, we do not consider the scenario with the oversaturated demand. In such scenarios, the food delivery supply is not sufficient in each batch-matching process which leads to significant delay and market failure. This assumption allows us to analyze under the guarantee of a sufficient source of food delivery supply so that the service quality is satisfactory. Besides, we assume fixed travel times, as justified by existing studies in on-demand mobilities (e.g., Yang et al., 2010; Zhang et al., 2023). The impact of food delivery flow on the congestion level is more complex than that of common traffic. In urban areas, delivery drivers usually ride e-bikes (such as in large metropolitan areas in North America and the majority of places, if not all of them, in East Asia) for delivery, and many places have dedicated lanes for non-motorized vehicles (Liu et al., 2021) and thus the delivery is not impacted by normal automobile traffic. While in suburban areas, the traffic is usually negligible. We therefore do not consider the congestion and leave it for future study.

5.1.1 Batch-matching problem with equilibrium constraints

We first formulate the matching problem of the food delivery platform. We consider a food delivery platform that employs a batch-matching process to pair awaiting vacant drivers with order bundles. This process first accumulates order bundles and vacant drivers within a time interval to form a batch, and subsequently, the system matches these batches of order bundles with vacant drivers to improve system-wide performance. From a merchant's perspective, there are multiple order bundles before matching, each of which contains several orders that could be from different locations or the same. For drivers, when they are assigned an order bundle, they follow the instructed delivery path (as defined in Definition 2) to deliver the orders one by one. Since there are multiple vacant drivers and order bundles accumulated, it is anticipated that performing batch-matching can potentially result in a better matching outcome compared with that under the first-come-first-served policy; some works in the literature of ride-sourcing have already studied the design of the matching time interval (e.g., Yang et al., 2020). In this work, we allow delivery drivers to be matched from

other locations (inter-regional matching) instead of restricting the matching within local regions. In practice, the first priority for matching is normally local drivers. However, there exist some scenarios where the number of vacant drivers in a region is not sufficient to meet the demand, which requires the platform to "borrow" some drivers from adjacent regions. This operation also helps to reposition some vacant drivers as known in the literature (e.g., Luo et al., 2023; Dong et al., 2024).

Let the distance between the drivers' and merchants' locations be $\mathbf{l}_{vm} = \{L_{vm} : v \in \mathcal{N}^{\text{dr}}, m \in \mathcal{N}^{\text{mer}}\}$, the distance between the customers' and merchants' locations be $\mathbf{l}_{cm} = \{L_{cm} : c \in \mathcal{N}^{\text{cus}}, m \in \mathcal{N}^{\text{mer}}\}$, $\mathbf{q}$ be the vector form of the customer demand rate $q_{c,m}$, and $\boldsymbol{\lambda}^{\mu}$ be the vector form of the matching flow λ^{μ}_{vm}. We consider that vacant drivers matched will be paid at w \$/km plus a base w_0 for their traveling for pickup, each customer will pay a fee of p \$/km to the platform for their food delivery service, and customers pay p_o on average for each order. We then consider the following cost function of batch-matching in Equation (1) (a minimizing problem so there is a minus sign):

$$f_{\mu}(\mathbf{q}, \boldsymbol{\lambda}^{\mu}) = -\left[\gamma p_o \mathbf{1}^{\top}\mathbf{q} + p\mathbf{l}_{cm}^{\top}\mathbf{q} - (w_0 + w\mathbf{l}_{vm}^{\top})\boldsymbol{\lambda}^{\mu}\right], \tag{24}$$

where $\gamma p_o \mathbf{1}^{\top}\mathbf{q}$ represents the commission charged to merchants on every purchase of order on the platform, $p\mathbf{l}_{cm}^{\top}\mathbf{q}$ represents the revenue of the delivery fee charged to customers, and $(w_0 + w\mathbf{l}_{vm}^{\top})\boldsymbol{\lambda}^{\mu}$ represents the wage paid to drivers for their pickup journey. Readers are directed to Table 4 for the meaning of each symbol. Equation (24) represents the revenue less the matching cost. Apart from the cost function, the feasible set of the matching flow $\mathcal{F}_{\mu}$ in Equation (1c) is defined by the following conditions:

$$\tau \sum_{v}\sum_{m} \lambda^{\mu}_{vm} = \sum_{m} m^{\text{cus}}_{m}, \tag{25}$$

$$\tau \sum_{v} \lambda^{\mu}_{vm} \leq m^{\text{cus}}_{m} : \forall m, \tag{26}$$

$$\tau \sum_{m} \lambda^{\mu}_{vm} \leq m^{\text{dr}}_{v} : \forall v, \tag{27}$$

where Equation (25) means that the total number of matched vacant drivers should be equal to the number of order bundles (since we assume the total number of order bundles is less than the total number of vacant drivers). This condition is also known as the market-clearing condition in the literature (Yang et al., 2010). Equations (26) and (27) ensure that the matched vacant vehicles or order bundles do not exceed the existing awaiting ones. As a result, the feasible set of the batch-matching problem $\mathcal{F}_{\mu} := \{\lambda^{\mu}_{vm} : \text{Equations (25) to (27)}\}$.

5.1.2 Delivery dispatching problem with order bundling

The second decision of the platform is the bundling delivery dispatching on determining the path flows, denoted $\boldsymbol{\lambda}^o_{\mathcal{P}}$. Unlike traditional vehicle routing problems, which aim to find the optimal sequence of routes, we consider this problem from a higher perspective, focusing on the vehicular flow of each delivery route. The central idea of this continuous approximation is not to determine the optimal visiting sequence, but to find the "best" route(s) among all possible routes and assign drivers to them.

The delivery paths and their length can be enumerated by computer algorithms, and they are exogenous, which means they are available once the geographical information of a studied region is known. In practice, the enumerating process can be done in reasonable times (say, several minutes using a laptop) if the bundling ratio is not very large and can be further accelerated by using parallel computing techniques. As for the bundling delivery dispatching problem, we shall first look into the number of decision variables. Let $\mathcal{N}^{\text{del}}_m$ denote the delivery area of merchants at m and $|\mathcal{N}^{\text{del}}_m|$ represents the number of potential customer locations within the delivery area. For any bundling ratio $k \leq \hat{k}$ of merchants at m, the set of all possible bundles of size k is denoted as $\mathcal{B}^k_m$, the total number of all possible bundles of all k's is obtained by $I_m = \sum_{k=1}^{\hat{k}} |\mathcal{B}^k_m|$. The cardinality $|\mathcal{B}^k_m|$ is obtained by a combinatorial number $|\mathcal{B}^k_m| = \binom{|\mathcal{N}^{\text{del}}_m| + k - 1}{k}$. This value is obtained by the following logic. We consider the number of possible order bundles as how many of combinations with repetitions (each element of the set can repeat) are there to take k nodes out of $|\mathcal{N}^{\text{del}}_m|$ nodes, and there are established theories to calculate this number (Brualdi, 2010, pp.168). For all merchants, the total number of delivery paths is $|\boldsymbol{\lambda}^o_{\mathcal{P}}| = \sum_m I_m$.

The delivery dispatching problem is to determine the optimal path flow of each delivery path, i.e., to solve for the decision variable $\boldsymbol{\lambda}^o_{\mathcal{P}}$. The optimization objective varies, for instance, reducing the delivery cost or reducing the customers' waiting time. On the other hand, it is also beneficial to investigate the scenario where the platform does not intervene in the delivery dispatching process so that we can know how much improvement the optimized operation can offer. In such a scenario, the order bundles are formed randomly, and the delivery drivers pick up whatever they obtain as soon as they arrive at the merchants. To sum up, we formulate and compare three different objectives for the bundling delivery dispatching problem: 1) a random-bundling strategy where there is no platform intervention, 2) a strategy on minimizing labor cost (and thus improving profit), and 3) a strategy on minimizing the customers' waiting time.

Apart from the decision variable of the delivery dispatching problem, we also look into the feasible set $\mathcal{F}_d$ in Equation (1d). The constraint defining $\mathcal{F}_d$ is merely the food delivery demand–supply equilibrium as we analyzed before in Sections 3 and 4.2. According to Equation (16), the demand–supply constraint yields $\mathcal{F}_d := \{\boldsymbol{\lambda}^o_{\mathcal{P}} : \mathbf{A}\boldsymbol{\lambda}^o_{\mathcal{P}} = \mathbf{q}\}$.

Random-bundling strategy (RBS). When the platform is not involved in delivery dispatching, the customer orders are randomly (spontaneously) formed as bundles and there is no pre-organization of the order bundles. As a result, each delivery path could happen at random and the objective function in Equation (1a) becomes solely $f_\mu(\mathbf{m}, \boldsymbol{\lambda}^\mu)$. We refer to this approach as RBS, an initialism for the random-bundling strategy. Unlike other strategies, the RBS does not necessitate an optimization process. However, during the evaluation phase, the profit is determined by subtracting the monetary delivery cost from f_μ, maintaining consistency with other strategies. The vehicular flows of each delivery path are be calculated in closed form to substitute f_d and $\mathcal{F}_d$, by the flow originating from a merchant multiplied by the probability of the appearance of each order bundle of that merchant:

$$\lambda^o_{m,i} = \lambda^o_m P(\mathcal{B}_{m,i}|m), \tag{28}$$

where $m \in \mathcal{N}^{\text{mer}}$, $i \in \mathcal{I}_m$, and $P(\mathcal{B}_{m,i}|m)$ denotes the probability of the appearance of each order bundle from each merchant based on customers' demand rate for that bundle. Considering there are different permutations of customers in a bundle, the probability $P(\mathcal{B}_{m,i}|m)$ is obtained by

$$P(\mathcal{B}_{m,i}|m) = |\mathcal{B}_{m,i}|_p \prod_{c \in \mathcal{B}_{m,i}} \frac{P(c,m)}{P(m)}, \tag{29}$$

where the probabilities $P(m)$ and $P(c,m)$ are obtained based on the demand rate: $P(c,m) = \frac{q_{c,m}}{\sum_c \sum_m q_{c,m}}$ and $P(m) = \frac{\sum_c q_{c,m}}{\sum_c \sum_m q_{c,m}}$; $|\cdot|_p$ calculates the number of unique permutations of each order bundle $\mathcal{B}_{m,i}$, which is

$$|\mathcal{B}_{m,i}|_p = \frac{k!}{\prod_{c \in \text{Unique}(\mathcal{B}_{m,i})} C(c, \mathcal{B}_{m,i})!}, \tag{30}$$

where $C(c, \mathcal{B}_{m,i})$ returns the number of c's in $\mathcal{B}_{m,i}$, and $\text{Unique}(\cdot)$ gives the unique elements in $\mathcal{B}_{m,i}$. For instance, an order bundle of merchant at node 1 contains $\{1,1,2,3\}$, then, $C(1, \{1,1,2,3\}) = 2$, $\text{Unique}(\{1,1,2,3\}) = \{1,2,3\}$, and $|\{1,1,2,3\}|_p = \frac{4!}{2! \cdot 1 \cdot 1} = 12$.

Delivery cost minimization strategy (DCS). In this strategy, the platform intervenes in the delivery dispatching process to reduce delivery costs. Since the batch-matching process has already aimed at improving profit, it is conceivable to consider reducing the labor cost in the delivery process so as to improve total profit. Under such a strategy, the vehicular flow of each delivery path is obtained by solving the SMD problem in Equation (1) with f_d^{DCS} in the following form,

and the strategy is called the delivery cost minimization strategy (DCS):

$$f_d^{DCS}\left(\lambda_{m,i}^o\right) = \overbrace{\sum_m \sum_{i\in\mathcal{I}_m} \lambda_{m,i}^o (w_0 k_{m,i} + w d_{m,i})}^{\text{labor cost: wage paid to delivery drivers}}, \tag{31}$$

where $k_{m,i}$ denotes the number of orders (bundling ratio) in the bundle i of merchants at m.

Let $\boldsymbol{\lambda}_{\mathcal{P}}^o$, $\mathbf{d}$, and $\mathbf{k}$ denote the vector form of $\lambda_{m,i}^o$, $d_{m,i}$, $k_{m,i}$, respectively, we have the following vector form of Equation (31):

$$f_d^{DCS}(\boldsymbol{\lambda}_{\mathcal{P}}^o) = (w_0 \mathbf{k}^\top + w \mathbf{d}^\top)\boldsymbol{\lambda}_{\mathcal{P}}^o. \tag{32}$$

Intuitively, to reduce the total driver wage cost, the strategy will assign drivers from the merchant to the closest possible customer and also try to avoid delivering customers from distant regions.

Waiting time minimization strategy (WTS). In ride-sourcing service, customers are subject to matching and pickup time, and the en-route trip time or delivery time (e.g., Ke et al., 2020a). In the context of food delivery service, there is another source of waiting time, namely the order accumulation time. This delay is one of the major differences between RS and OFD services because of the order bundling in OFD services. The accumulation time is the duration during which a full bundle is formed. Therefore, customers' waiting time consists of four parts: matching time, pickup time, delivery time, and accumulation time. Among them, the matching time and the pickup time are not directly influenced by the delivery path flow, whereas the other two are. Therefore, the focus on reducing customers' waiting time moves to the minimization on the order accumulation time and delivery time.

For each order bundle, the order accumulation time is how long it will take to form an order bundle. The accumulation time of each order bundle is

$$W_{m,i}^a := \max\left(\left\{\frac{C(c,\mathcal{B}_{m,i})}{q_{c,m}} : c \in \mathcal{B}_{m,i}\right\}\right), i \in \mathcal{I}_m, \tag{33}$$

where $C(c,\mathcal{B}_{m,i})$ is a function returning the number of c's in a bundle $\mathcal{B}_{m,i}$. Then, let $\mathbf{q}_{\mathcal{P}} \equiv \boldsymbol{\lambda}_{\mathcal{P}}^o \odot \mathbf{k}$ be the demand rate for each delivery path where $\odot$ denotes the element-wise multiplication (also known as Hadamard product) and $\mathbf{k}$ denotes the vector of the number of orders in each bundle (each element of $\mathbf{k}$ should be less than or equal to the bundling capacity $\hat{k}$). The average order accumulation time W^a is calculated by the average of the accumulation time of paths weighted by $\mathbf{q}_{\mathcal{P}}$. Since Equation (33) contains $q_{c,m}$, W^a can be considered as a function of $q_{c,m}$. Given $q_{c,m}$ and

then $\mathbf{q}$, let $\mathbf{w}_a$ be the vector of $W^a_{m,i}$ dependent on $\mathbf{q}$ so $\mathbf{w}_a = \mathbf{w}_a(\mathbf{q})$, W^a is computed by

$$W^a = \left(\frac{\mathbf{q}_{\mathcal{P}}}{\mathbf{1}^\top \mathbf{q}_{\mathcal{P}}}\right)^\top \mathbf{w}_a(\mathbf{q}), \tag{34}$$

where $\frac{\mathbf{q}_{\mathcal{P}}}{\mathbf{1}^\top \mathbf{q}_{\mathcal{P}}}$ represents the probability of appearance of each delivery path. By some simple algebraic manipulation, we have the following linear transformation for $\boldsymbol{\lambda}^o_{\mathcal{P}}$,

$$W^a = \left(\frac{\mathbf{w}_a(\mathbf{q}) \odot \mathbf{k}}{\mathbf{1}^\top \mathbf{q}}\right)^\top \boldsymbol{\lambda}^o_{\mathcal{P}}, \tag{35}$$

where $\mathbf{1}^\top \mathbf{q}$ means the summation of all elements in the vector $\mathbf{q}$.

From Claim 1, we know that given $\mathbf{q}$, the average delivery time is a linear transform from $\boldsymbol{\lambda}^o_{\mathcal{P}}$. Then, we are ready to present the cost function of the waiting time minimization strategy (WTS). Since Equation (24) considers the total revenue, we multiply W^a and W^{cd} by $\sum_c \sum_m q_{c,m} \equiv \mathbf{1}^\top \mathbf{q}$ and multiply by value of time:

$$f_d^{WTS} = \beta \left[\mathbf{1}^\top \mathbf{M}^{cd} + (\mathbf{w}_a(\mathbf{q}) \odot \mathbf{k})^\top\right] \boldsymbol{\lambda}^o_{\mathcal{P}}, \tag{36}$$

where β is the value of time coefficient to keep f_d in monetary unit.

5.2 The SMD problem with equilibrium constraints

The stationary matching and dispatching (SMD) problem introduced in Section 3 is now ready to be presented with three different delivery dispatching strategies. Let EQ, BM, and BDD denote, respectively, the initialisms of equilibrium, batch-matching, and bundling delivery dispatching.

SMD with RBS. From Equation (1) and the batch-matching objective Equation (24), we have

$$\begin{aligned} \min_{\mathbf{m}, \boldsymbol{\lambda}^\mu,} \quad & \overbrace{-\left[\gamma p_o \mathbf{1}^\top \mathbf{q} + p \mathbf{l}_{cm}^\top \mathbf{q} - (w_0 + w \mathbf{l}_{vm}^\top) \boldsymbol{\lambda}^\mu\right]}^{f_\mu(\mathbf{m}, \boldsymbol{\lambda}^\mu)} \\ \text{s.t.} \quad & \text{EQ constraints: Equation (23),} \\ & \text{BM feasibility: Equations (25) to (27),} \end{aligned}$$

where $\boldsymbol{\lambda}^o_{\mathcal{P}}$ is solved by Equations (28) to (30).

SMD with DCS. From Equations (1), (16), (24) and (32), we have

$$\min_{\mathbf{m}, \boldsymbol{\lambda}^\mu, \boldsymbol{\lambda}^o_{\mathcal{P}}} \quad \overbrace{-\left[\gamma p_o \mathbf{1}^\top \mathbf{q} + p \mathbf{l}_{cm}^\top \mathbf{q} - (w_0 + w \mathbf{l}_{vm}^\top) \boldsymbol{\lambda}^\mu\right]}^{f_\mu(\mathbf{m}, \boldsymbol{\lambda}^\mu)} + \overbrace{(w_0 \mathbf{k}^\top + w \mathbf{d}^\top) \boldsymbol{\lambda}^o_{\mathcal{P}}}^{f_d(\boldsymbol{\lambda}^o_{\mathcal{P}})}$$

s.t. EQ constraints: Equation (23),

BM feasibility: Equations (25) to (27),

BDD feasibility: $\mathbf{A}\boldsymbol{\lambda}_{\mathcal{P}}^{o} = \mathbf{q}$.

SMD with WTS. From Equations (1), (16), (24) and (36), we have

$$\min_{\mathbf{m},\boldsymbol{\lambda}^{\mu},\boldsymbol{\lambda}_{\mathcal{P}}^{o}} \overbrace{-\left[\gamma p_o \mathbf{1}^{\top}\mathbf{q} + p\mathbf{l}_{cm}^{\top}\mathbf{q} - (w_0 + w\mathbf{l}_{vm}^{\top})\boldsymbol{\lambda}^{\mu}\right]}^{f_{\mu}(\mathbf{m},\boldsymbol{\lambda}^{\mu})} + \overbrace{\beta\left[\mathbf{1}^{\top}\mathbf{M}^{cd} + (\mathbf{w}_a(\mathbf{q}) \odot \mathbf{k})^{\top}\right]\boldsymbol{\lambda}_{\mathcal{P}}^{o}}^{f_d(\mathbf{m},\boldsymbol{\lambda}_{\mathcal{P}}^{o})}$$

s.t. EQ constraints: Equation (23),

BM feasibility: Equations (25) to (27),

BDD feasibility: $\mathbf{A}\boldsymbol{\lambda}_{\mathcal{P}}^{o} = \mathbf{q}$.

5.3 Solution algorithm

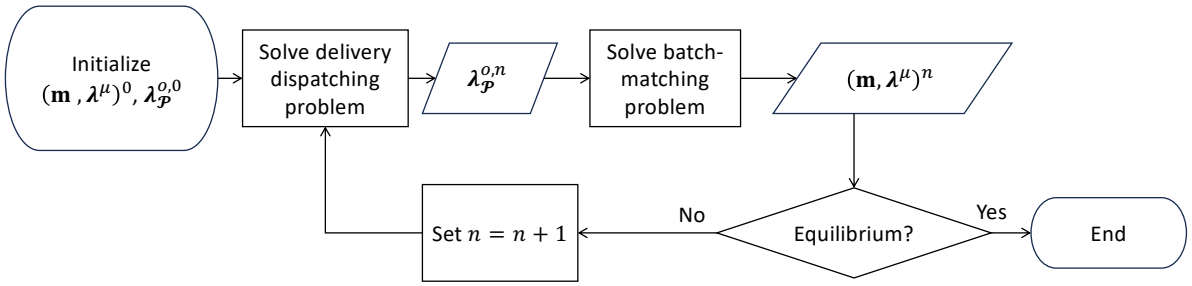

Figure 4: Flowchart of the solution algorithm.

For small networks and small bundling ratios, the SMD problems can be solved directly using commercial software such as MATLAB (the built-in function *fmincon* are designed to solve constrained optimization problems). However, for large-scale networks, the problem is harder to solve because of the equilibrium constraints, the logit-based choice model, and the formulation of the probability-based delivery path flow in RBS which involves many nonlinear even nonconvex terms. We then approximate the original problem by its decomposition and use an iterative heuristic algorithm to solve the decomposed SMD problem, which we consider the coordinate descent (CD) algorithm (Wright, 2015). In this study, the subproblems are the batch-matching problem and the bundling delivery dispatching problem. The algorithm solves SMD by taking the results of one subproblem as the input to the other. By doing so, the delivery dispatching becomes a linear programming problem because the customer demand becomes constant in the subproblem. Therefore, even though the bundling capacity is large, which leads to many delivery paths, the subproblem can still be solved efficiently. On the other hand, the batch-matching problem is also easier to solve because the delivery path flow is fixed within the subproblem. The algorithm converges to

a steady-state solution if the demand is not excessively large, which is one of our assumptions, representing a reachable demand–supply equilibrium of the market. Our attempt to solve for a large-scale network in the numerical study also demonstrates the convergence of our algorithm. Numerical experiments demonstrate that the decomposed SMD solutions comply with the original problem constraints, with a sum of squares of violations at a scale of 1×10^{-4} on average, which allows us to substitute the SMD solution with the solution of the decomposed SMD problem.

Let n and $n+1$ on the superscript denote the count of iterations, the algorithm (see flowchart in Figure 4) starts with an initial point $\mathbf{m}^0$, $\boldsymbol{\lambda}_{\mathcal{P}}^{o,0}$, and $\boldsymbol{\lambda}^{\mu,0}$ and updates each iteration as follows until two contiguous iterations produce results within tolerance and the first-order optimality is met.

[Decomposed SMD]

$$\boldsymbol{\lambda}_{\mathcal{P}}^{o,n+1} = \text{argmin}_{\boldsymbol{\lambda}_{\mathcal{P}}^{o}} \{f_d(\boldsymbol{\lambda}_{\mathcal{P}}^{o}, \boldsymbol{\lambda}^{\mu,n}, \mathbf{m}^n) : \boldsymbol{\lambda}_{\mathcal{P}}^{o} \in \mathcal{F}_d(\boldsymbol{\lambda}^{\mu,n}, \mathbf{m}^n)\}, \tag{40a}$$

$$(\mathbf{m}, \boldsymbol{\lambda}^{\mu})^{n+1} = \text{argmin}_{\boldsymbol{\lambda}^{\mu}} \left\{ f_\mu(\boldsymbol{\lambda}^{\mu}, \mathbf{m}) : \mathbf{m} \in \mathcal{S}_e\left(\boldsymbol{\lambda}^{\mu}, \boldsymbol{\lambda}_{\mathcal{P}}^{o,n+1}\right) \text{ and } \boldsymbol{\lambda}^{\mu} \in \mathcal{F}_\mu(\mathbf{m}) \right\}. \tag{40b}$$

6 Numerical study on Grubhub data

This section presents numerical studies for the three-sided network equilibrium. The numerical study uses the dataset provided by Grubhub which is a large food delivery company in the US (Reyes et al., 2018). Also, we show how the platform's operations on delivery dispatching benefit either the platform's profit or the customers' waiting time. We then provide sensitivity analyses on the impacts of the bundling ratio, vehicle fleet size, and pricing policies (i.e., delivery fee, wage, and commission) to three market players by analyzing performance metrics.

6.1 Experiment setup

We first demonstrate how to translate our model into real practice. Although some classical networks, such as the Sioux Falls network, appear to be popular in transportation engineering research, these networks were initially for traffic flow assignment usage instead of service network design, not to mention that these networks and the involved data are all synthetic data. Considering that there is a public dataset from a well-known company, we decided to use the real-world data and partition the involved region into a network topology. The numerical study is based on the dataset provided by Grubhub and the dataset was initially introduce by Reyes et al. (2018) on the meal delivery routing problem (MDRP). The dataset provides information such as order placement and driver work schedule, allowing us to derive delivery demand and fleet information based on the dataset. The geographical distribution of orders is shown in Figure 5a where we perform the K-

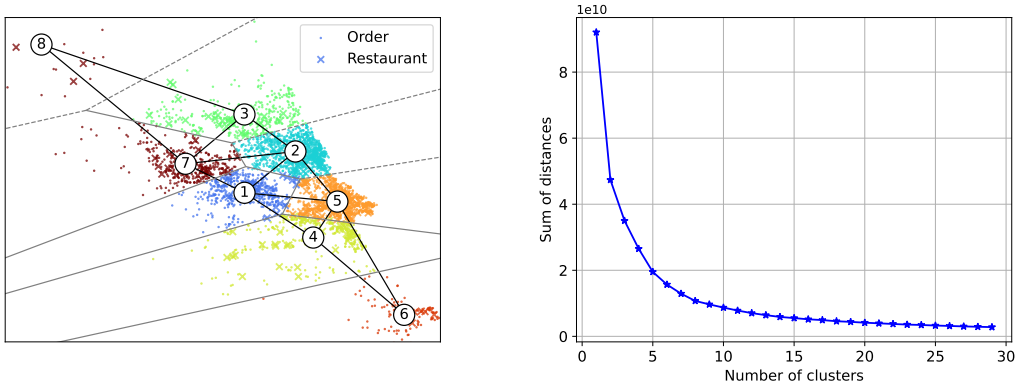

(a) Grubhub network.

(b) K-Means clusters.

Figure 5: Grubhub network partitioning using K-Means

Means clustering method to partition the area into several regions. The partitioning metrics are the geographical coordinates and the number of restaurants surrounded (here we use the number of restaurants within a radius of 1 km). We then connect the adjacent regions and form a network topology of the studied region. The number of clusters is selected based on the sum of squares of the distance to the cluster center which is a simple yet standard selection criterion when using K-Means clustering. We decide to partition the region into 8 regions based on the curve shown in Figure 5b, because there is no significant benefit of reducing the sum of distance squares to further increase the number of clusters. To demonstrate the capability of our solution algorithm on its potential for solving larger-scale networks, we also solve for the partition with 20 regions, where the number of decision variables of delivery paths increases from 2314 to 27024, and the number of unknown variables (solved from the equilibrium conditions) increases from 88 to 460. Although the number of decision variables in total increases significantly, our solution algorithm can still produce the solution within a reasonable time, and the sum of squares of the numerical violation of constraints is negligible, providing a strong feasibility of the results. Therefore, it demonstrates the scalability and efficiency of our solution method. We show in Appendix H to illustrate the network flow for drivers and customers. Due to the limitation of space, unless otherwise stated, this section will present the numerical experiments conducted on a network comprising eight regions. We believe this configuration adequately represents an average-scale town as illustrated in the Grubhub dataset.

The settings of the exogenous variables are listed in Table 1. Also, the vehicle fleet size and customer demand are analyzed based on one of the Grubhub dataset samples. All the locations are considered part of the matching area and there are merchants within each region, and the delivery area is set to be the second-order neighborhood of each merchant. Unless otherwise specified, we use the default values $\hat{k} = 4$, $\hat{N}_F = 600$, $\gamma = 0.2$, $w = 3$, and $p = 5$, respectively. The behavioral coefficients of customers, vacant drivers, and merchants are listed here for reproducibility of our

Table 1: Numerical study settings.

Symbols	Unit	Values
β	[\$/hr]	20
v	[km/hr]	15
t_s	[hr]	0.1
τ	[hr]	0.001
w_0	[\$]	1
w	[\$/km]	3
p_o	[\$]	25
p	[\$/km]	5
γ	/	0.2

results: $\theta^{\text{cus}} = 0.1$, $\theta^{\text{cus},a} = 0.0005$, $\theta^{\text{dr}} = 0.0001$, and $\theta^{\text{dr},a} = 0.01$. These experiment settings are exclusively for illustrating purposes, especially the coefficients of behavioral models. In practice, decision-makers may need to collect more real-world data and also calibrate the coefficients of the driver/customer/merchant behavioral models based on local conditions.

6.2 Benefit of the platform's operations in delivery dispatching

The operational strategy first brings differences to the realized vehicle fleet. Note that the term "delivery supply" is used to describe the ability of delivering food by the realized fleet, then it is directly influenced by both vehicle fleet size and bundling capacity. We compare two market scenarios in Figure 6 showing the composition of three types of drivers for three delivery dispatching strategies, where on the left it is under a sufficient delivery supply ($\hat{N}_F = 600$ and $\hat{k} = 4$) while on the right it is under an insufficient delivery supply ($\hat{N} = 470$ and $\hat{k} = 3$), all others being equal. Note that the label "vacant" in Figure 6 stands for those drivers on their way to a waiting point, and only those drivers "awaiting" are eligible for matching.

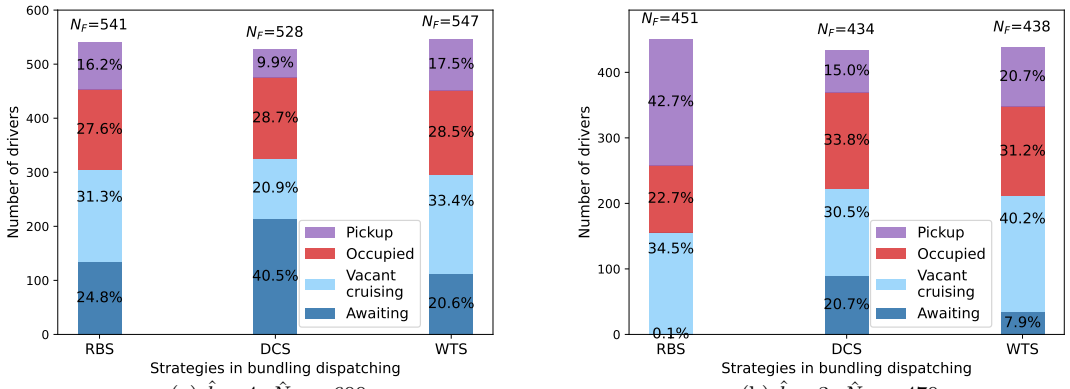

(a) $\hat{k} = 4$, $\hat{N}_F = 600$ (b) $\hat{k} = 3$, $\hat{N}_F = 470$

Figure 6: Allocation of drivers

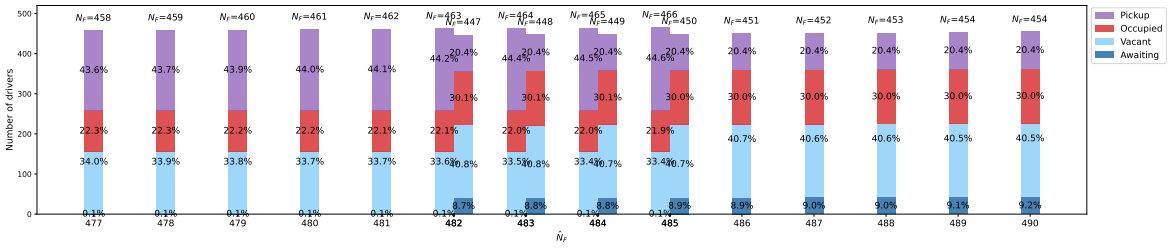

Figure 7: Allocation of driver with different $\hat{N}_F$ under RBS

According to Figure 6, the realized vehicle fleet is smallest under DCS in both scenarios. The mechanism is straightforward, i.e., by lowering total delivery cost, DCS suppresses driver earnings and thus the supply of participating drivers. For the platform, a smaller active fleet reduces labor expenditure and can raise profit. When delivery supply is scarce, the non-intervention baseline (RBS) produces a large mass of drivers traveling to pickups rather than delivering. This reproduces the "Wild Goose Chase" failure documented by Castillo et al. (2025), where drivers spend substantial time deadheading to pickups, leaving very few immediately available for matching in our experiments. Figure 7 plots driver counts by status against fleet size, under RBS dispatching, showing that this fragile regime arises primarily under low supply and that, for some fleet sizes, multiple equilibria can occur. By contrast, DCS and WTS tend to sustain a small but positive pool of waiting drivers eligible for assignment, preventing collapse into a pickup-dominated state. Shown in Figure 6, there are pools of awaiting drivers under DCS and WTS who are eligible for new order assignment. Therefore, platform intervention improves market robustness.

Table 2 reports waiting-time components across demand–supply conditions. With sufficient delivery supply, the matching queue clears each interval and the expected matching time is negligible for all strategies, which is consistent with queueing theory and prior models (Zhang et al., 2025). In contrast, under supply shortage the non-intervention baseline (RBS) exhibits large matching and pickup times because few drivers are immediately available. In other words, the market does not clear which leads to a large amount of matching time. Platform interventions (DCS and WTS) stabilize the system in this regime, yielding more reliable profit and customer waiting times.

Table 2: Comparison of waiting times across delivery dispatching strategies.

	Sufficient delivery supply			Insufficient delivery supply		
Metrics \ Strategies	RBS	DCS	WTS	RBS	DCS	WTS
Customer waiting time [hr]	0.51	0.47	0.40	1.17	0.46	0.42
Accumulation time [hr]	0.12	0.19	0.08	0.10	0.15	0.09
Matching time [hr]	0.0005	0.0003	0.0005	0.36	0.0004	0.0005
Pickup time [hr]	0.20	0.10	0.12	0.52	0.19	0.21
Delivery time [hr]	0.19	0.18	0.20	0.19	0.12	0.13

Also, Table 2 shows that, under sufficient delivery supply, WTS produces the lowest total customer waiting time relative to RBS and DCS. A decomposition of waiting times indicates that the improvement comes primarily from shorter accumulation time (faster bundle formation), while other components are comparable or only slightly affected. Thus, WTS improves service level chiefly by reducing pre-match congestion.

Table 3 shows more metrics other than waiting times. Platform profit rises substantially under DCS compared with RBS, as shown in . The gain is driven by higher revenue induced by shorter delivery times and the resulting demand increase, and by lower repositioning cost. Profit under DCS also exceeds WTS, mainly because DCS further reduces repositioning (inter-nodal pickup flow) and, to a lesser extent, delivery cost. Total customer demand is highest under DCS. By Equation (2), demand responds to matching and delivery times, both of which are smallest with DCS. Although WTS minimizes total waiting time, its advantage stems mostly from accumulation time, which customers do not directly perceive in the app; accordingly, it does not translate into higher demand. Drivers' hourly earnings are lowest under DCS and highest under WTS. The predicted earnings are consistent with external evidence (about \$23/hour in the United States; Indeed, 2025). The bundling ratio is also highest under DCS where bundles are larger yet predominantly concentrated within one or two regions (Table 6 in Appendix G).

Table 3: Comparison across delivery dispatching strategies.

Metrics \ Strategies	RBS	DCS	WTS
Customer waiting time [hr]	0.51	0.47	0.40
Platform profit [\$/hr]	3773	10310	6363
• Revenue [\$/hr]	15785	20819	19165
• Driver wage cost [\$/hr]	7607	7865	8014
• Reposition cost [\$/hr]	4405	2644	4788
Total customer demand [/hr]	877.2	1046.7	985.6
Total number of merchants	230.7	244.2	221.8
Realized vehicle fleet	541	528	547
Driver hourly earnings [\$/hr]	22.2	19.9	23.4
Average bundling ratio	1.92	3.60	2.10

6.3 Spatial distribution of flows

Figure 8 shows that the flow under RBS is amortized, but the flows are concentrated under DCS and WTS. In other words, only a handful of delivery paths are assigned with occupied drivers for each merchant under DCS and WTS. In Appendix G, we list the flow of each delivery path and the sequence of delivery order. It is shown that WTS tend to produce small bundles, where single orders are often, consistent with its reduction in accumulation time and its higher earnings. While

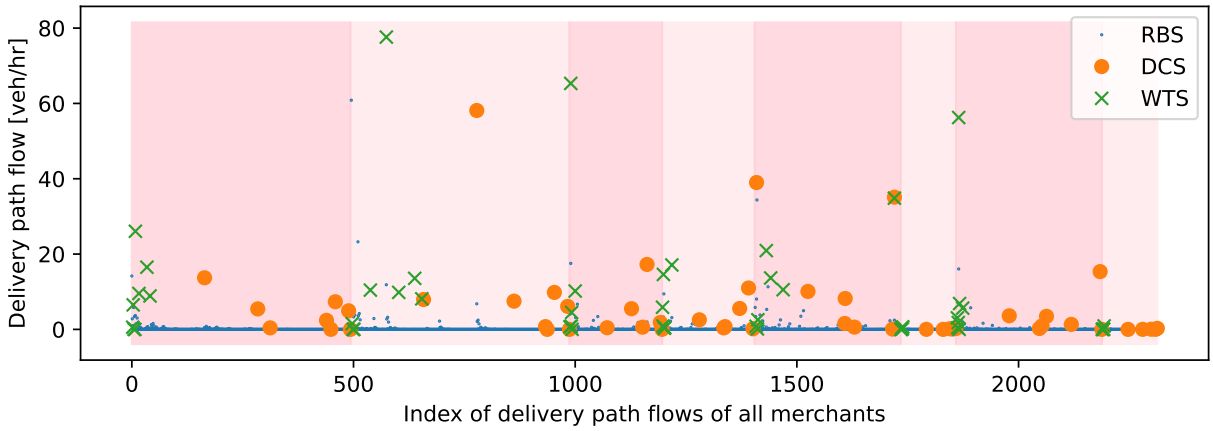

Figure 8: Delivery path flows (each pink block represents the coverage of a region).

under DCS, the orders bundled are concentrated in similar regions. We interpret this effect that bundling the orders sharing the same OD is the most ideal case but not always possible in practice, because of the demand–supply equilibrium constraint. This assignment preference also reduces the accumulation time because customers do not need to wait for those who are from other regions (these demands are typically smaller compared with local demand).

We provide the network structure of flows in Figures 9 to 11, where we visualize the spatial distribution of flows under three bundling dispatching strategies: random bundling (RBS), delivery cost minimization (DCS), and waiting time minimization (WTS). In Figures 9 to 11 , panel (a) displays the multi-stop delivery path flows $\lambda^{o}_{m,i}$ up to four stops which is the bundling capacity we used in this numerical study; panels (b)–(d) report the realized customer demand $q_{c,m}$, the matching flow λ^{μ}_{vm}, and the vacant-vehicle flow λ^{φ}_{cv}, respectively. A common baseline observation reveals that, in all strategies, panels (b)–(d) concentrate on local matching. The distinction appears in panel (a). Under RBS, ribbons are numerous and diffuse, indicating broad mixing of intermediate stops which is conceivable for a random-bundling strategy. In contrast, DCS and WTS compress the ribbons into a limited set of high-throughput corridors. This concentration is consistent with their objectives, i.e., minimizing wage cost or minimizing customer waiting time, which naturally produces geographically compact delivery sequences.

First, path lengths differ across policies. Under DCS and WTS the paths are largely reduced to within one or two geographical regions, with only a thin residual directed to third or fourth stops. Note that we consider, say, a bundle $\{1, 2, 2\}$ being within two regions but the bundling ratio is 3. RBS, by contrast, sustains a much heavier long tail of 3–4 stop sequences. This difference matters operationally, shorter tours reducing delivery time and improving service quality.

Second, the platform's intervention provides less inter-regional travel which contributes to shorter delivery time, among others, where the average number of geographical locations visited by drivers during delivery are 1.56, 1.53, and 1.41, respectively, for RBS, DCS, and WTS. There-

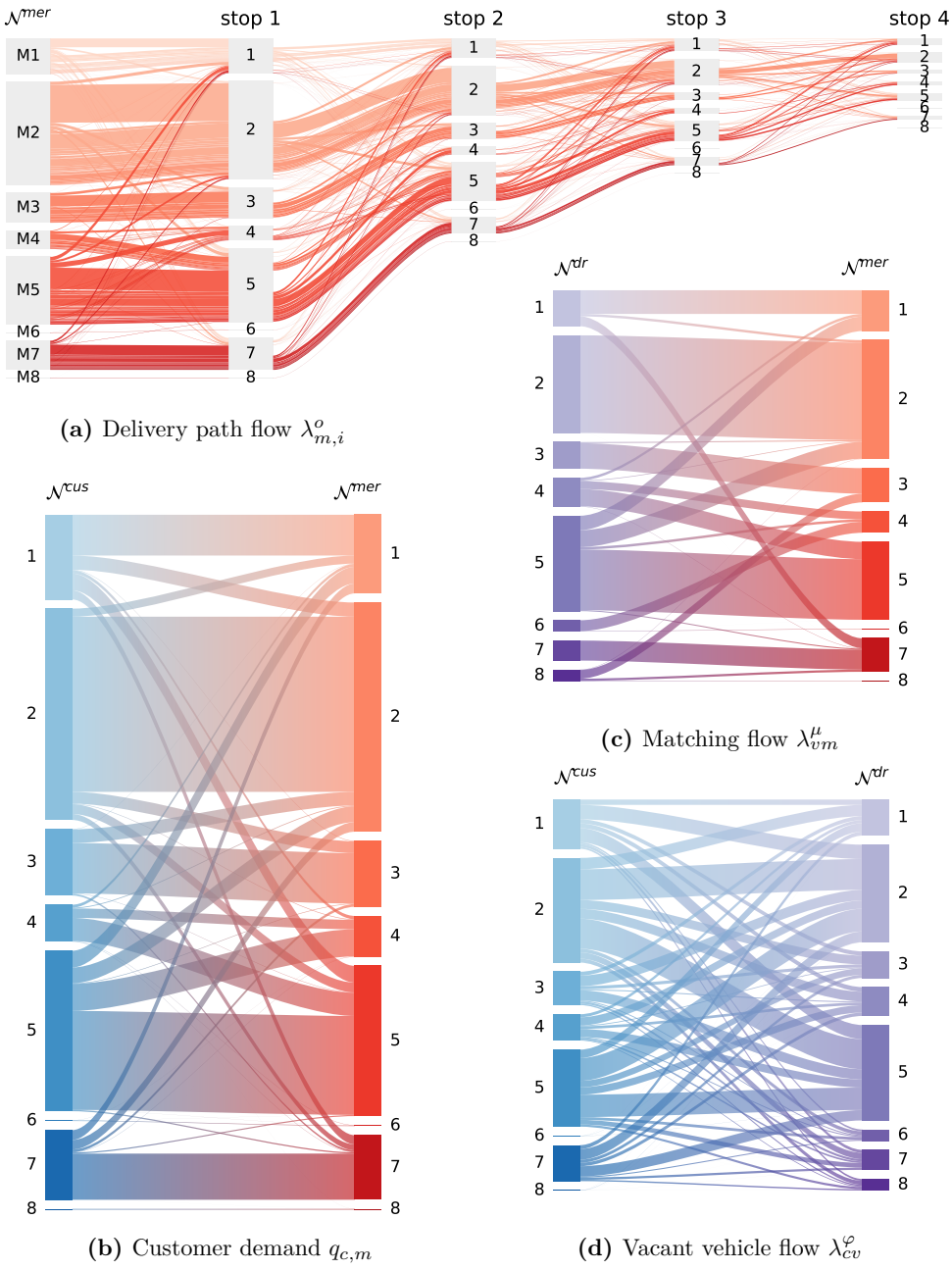

(a) Delivery path flow $\lambda^{o}_{m,i}$

(c) Matching flow λ^{μ}_{vm}

(b) Customer demand $q_{c,m}$

(d) Vacant vehicle flow λ^{φ}_{cv}

Figure 9: Flow distribution under random-bundling strategy (RBS)

fore, DCS and WTS produce a small number of stable corridors with limited cross-over, while RBS exhibits frequent crossings between intermediate stops. The former implies predictable, high-throughput lanes that can be explicitly supported by practical regulations (e.g., by micro-zones or dedicated delivery), whereas the latter implies dispersed traffic with higher pickup distance and uncertainty. These path-level distributions cannot be inferred from aggregate utilization alone while easy to analyze using our network model.

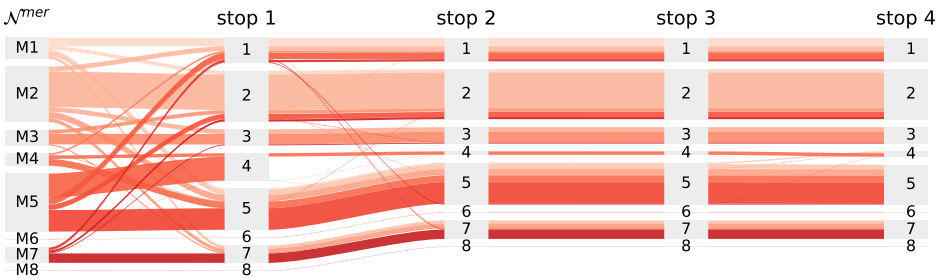

(a) Delivery path flow $\lambda^{o}_{m,i}$

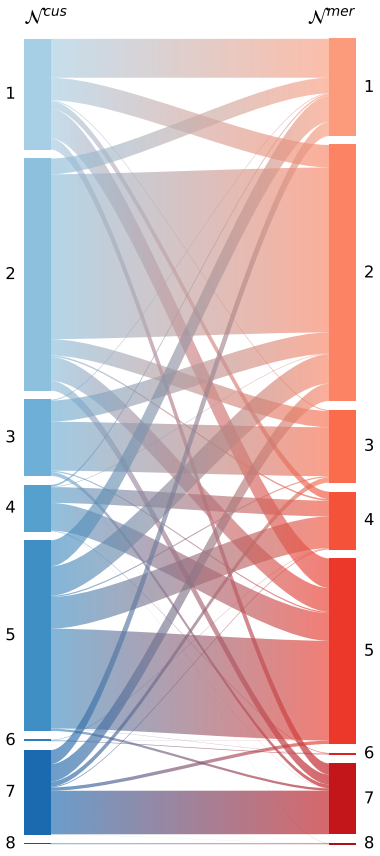

(b) Customer demand $q_{c,m}$

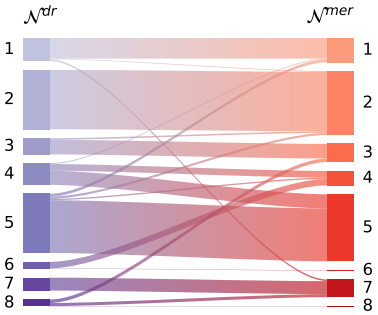

(c) Matching flow λ^{μ}_{vm}

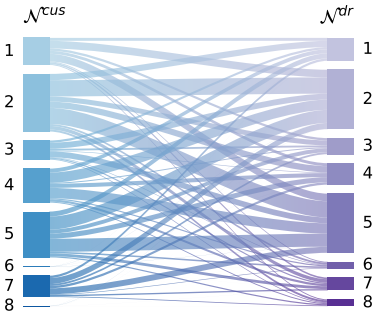

(d) Vacant vehicle flow λ^{φ}_{cv}

Figure 10: Flow distribution under delivery cost minimization strategy (DCS)

Third, the figures reveal a clear downstream propagation of early choices, a network effect. When policy concentrates flow on the first stop of a path, that concentration persists to later stops, propagating to the occupancy of downstream nodes and, ultimately, the realized demand $q_{c,m}$. The effect is most visible under DCS and WTS. It reinforces a small set of first-leg pairings, yielding high-throughput, steady corridors for supply flows. This propagation has the ability to couple matching (panel c), repositioning (panel d), and demand realization (panel b). For practitioners, by altering early stops of paths, the system could indirectly move where vehicles will next be free and where demand will be effectively served. This interdependence substantiates the value of the

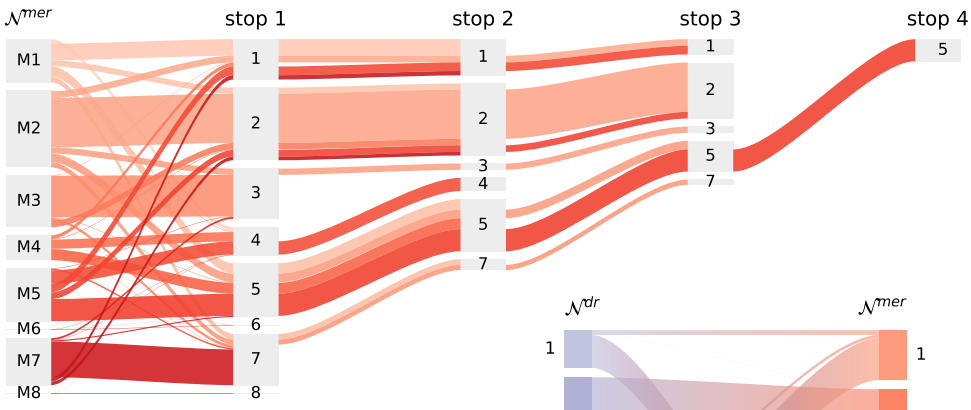

(a) Delivery path flow $\lambda^{o}_{m,i}$

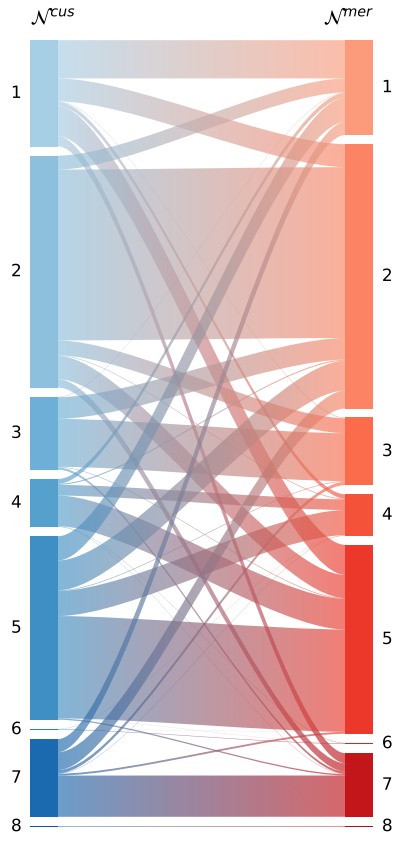

(b) Customer demand $q_{c,m}$

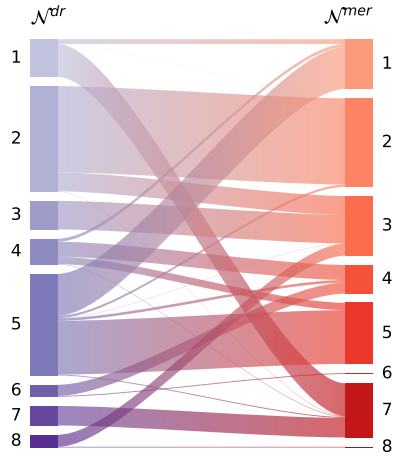

(c) Matching flow λ^{μ}_{vm}

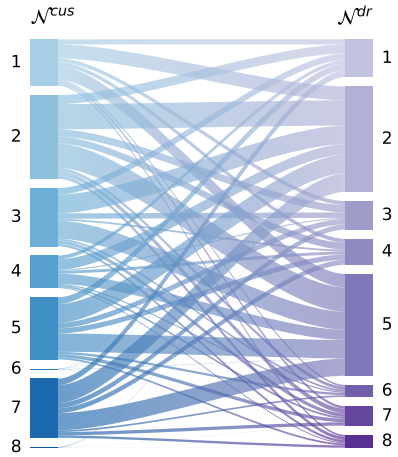

(d) Vacant vehicle flow λ^{φ}_{cv}

Figure 11: Flow distribution under waiting time minimization strategy (WTS)

network model, which captures how local policy at the first stop reorganizes the entire chain of the feedback loop.

6.4 Impacts of the bundling capacity and total vehicle fleet size

Figure 12 shows the impact of the bundling capacity $\hat{k}$ and the total vehicle fleet size $\hat{N}_F$ on 6 metrics. The impact of total fleet size is simpler than that of bundling capacity. In most cases, it influences the number of awaiting drivers and thus impact on the customer end. From the figure, we can see that the influences of $\hat{N}_F$ are typically monotonic. When $\hat{k} = 3$ and $\hat{N} = 470$, it is apparent that the market is experiencing an unhealthy condition (dashed line), as evidenced by the fact that few drivers are available for matching (Figure 12.e). In general, under the current experiment setting, these metrics hold a monotonic relationship with $\hat{k}$ under RBS and DCS, with some exceptions being non-monotonic under RBS such as total customer demand. Under WTS, these metrics are typically insensitive to $\hat{k}$. This can be attributed to the small-bundle strategy, as we discussed earlier in Section 6.2, which makes the bundling capacity non-influential.

Under RBS, sometimes the metrics are non-monotonic with respect to $\hat{k}$, such as customer waiting time and total demand. The bundling capacity $\hat{k}$ has a direct impact on these metrics under RBS because order bundling happens randomly, which means that every delivery path is possible to occur. In terms of total demand, as $\hat{k}$ increases, the customer demand first increases because larger bundling capacity helps serve more demands. However, it ends up with a decreasing effect because a large bundling ratio essentially increases delivery time and, in turn, reduces the total demand. This effect is not pronounced in the current setting, and only at high fleet size the non-monotone trend can be observed. We interpret it as the influence of the supply sufficiency. Intuitively, increasing the bundling capacity would contribute to the delivery supply, but it would negatively impact the service quality, leading to a decrease in demand. If the delivery supply is sufficient already (e.g., the vehicle fleet is large), the negative impact would occur more "quickly;" otherwise, the negative impact would not present.

The relationships between metrics and $\hat{k}$ are monotonic under DCS. Here, since $\hat{k}$ denotes the bundling capacity, the actual bundling ratio is not necessarily equal to $\hat{k}$, and through our experiment, they are actually very different (see Figure 12.d). As $\hat{k}$ increases, those paths under small $\hat{k}$'s are also included in the set of all paths. If $\{\mathcal{B}\}^{\hat{k}}$ denotes the set of all the order bundles with bundling capacity $\hat{k}$, we have $\{\mathcal{B}\}^{\hat{k}_1} \subset \{\mathcal{B}\}^{\hat{k}_2}$ for $\hat{k}_1 < \hat{k}_2$. Therefore, increasing $\hat{k}$ leads the market to a single direction, which is typically towards a better situation (in terms of the objective function) since the decision space is larger. The driver earnings decrease with $\hat{k}$ because as bundling capacity increases, the platform has more degrees of freedom to reduce the delivery cost and thus leads to less driver earnings. This also reflects a negative impact on the driver's welfare (surplus).

6.5 Impact of the pricing strategy on the three-sided market

Figure 13 depicts the sensitivity analysis of the pricing strategies on the three-sided market, namely 1) the delivery fee p charged to customers, 2) the wage w paid to delivery drivers, and 3) the revenue

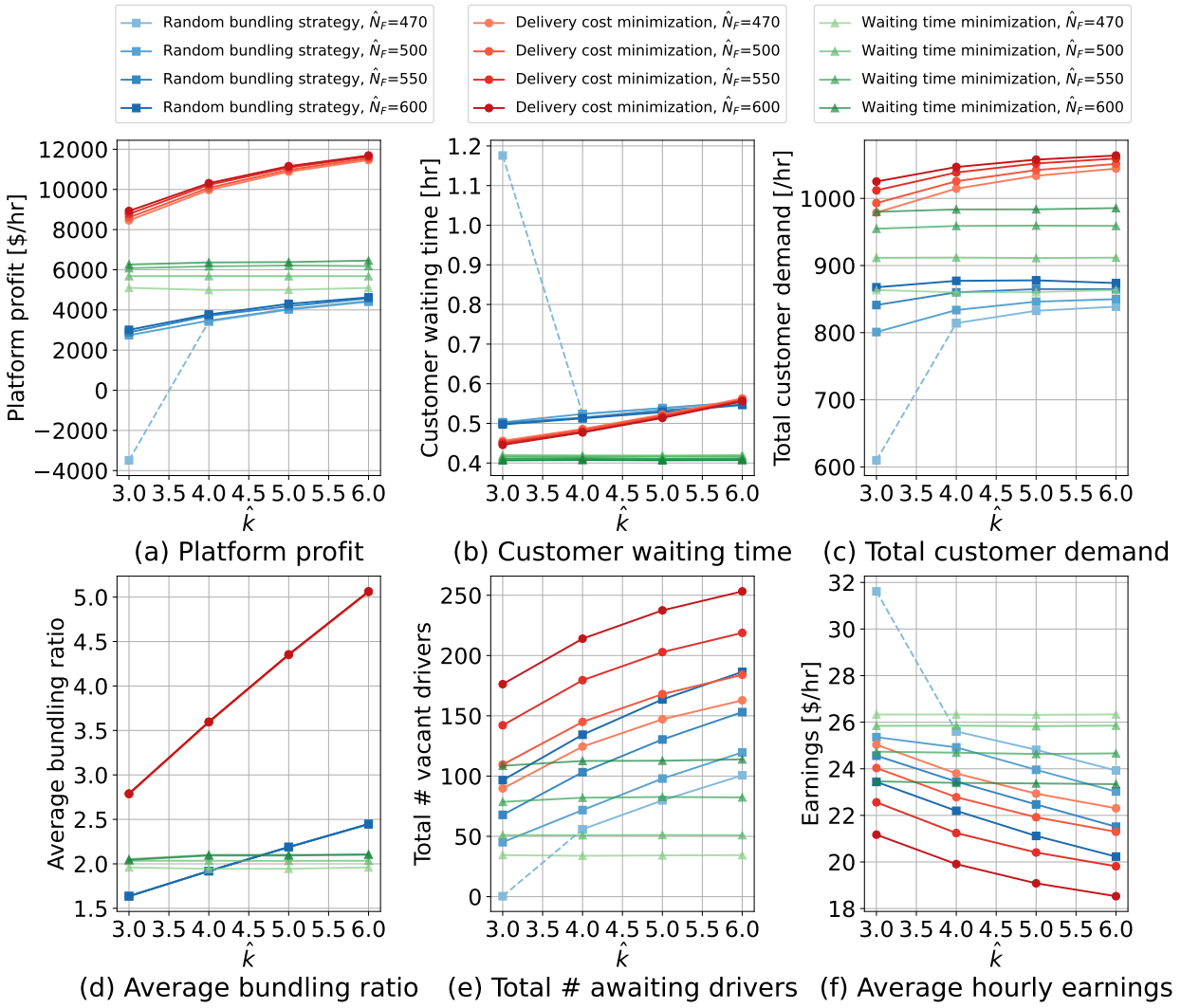

Figure 12: Impact of k and $\hat{N}_F$ on system metrics.

commission γ charged to merchants. These pricing strategies are imposed on each player, but they can impact all the players in the market. It is realized by the three-sided equilibrium where all the players are endogenously interconnected. To showcase the impact of customer demand on merchant behavior, we slightly increase the corresponding parameter. The dashed lines indicate the scenarios with an unbalanced demand–supply relationship, under which there is no steady state under the RBS dispatching strategy. In the horizontal direction, there are five metrics, which are the platform profit, customer waiting time, total customer demand, realized fleet size, and the number of merchants that are willing to be online on the platform. The first two metrics are key performance metrics for platform operators, while the last three metrics endogenously reflect the behavior of three market players. In the vertical direction, there are different pricing strategies where we take $w = 3$, $p = 5$, and $\gamma = 0.2$ as benchmark values and conduct comparative analyses. In the first row of subfigures, we increase w and fix $(p, \gamma) = (5, 0.2)$; the second row we increase p

and fix $(w,\gamma) = (3, 0.2)$; the third row we increase γ and fix $(w,p) = (3,5)$.

The first and second rows of Figure 13 clarify the impact of the distance-based wage w and the distance-based delivery fee p. The first row shows a monotonic effect of increasing w where higher wages raise drivers' earnings, thus enlarging the realized fleet. Changes in w primarily influence driver participation and customer waiting time, which then propagate to customer demand and merchant participation. On the customer side, better service translates into higher demand and shorter waiting times. On the merchant side, the greater reliability of pickup and delivery encourages more merchants to go online, increasing the active merchant count. These effects are system-wide, not limited to drivers. The second row, examined jointly with the first, highlights that the wage–fare relationship must respect $w < p$ and even with a considerable gap. For a large p, especially under WTS, its impact to profit becomes negative due to the decrease in customer demand.

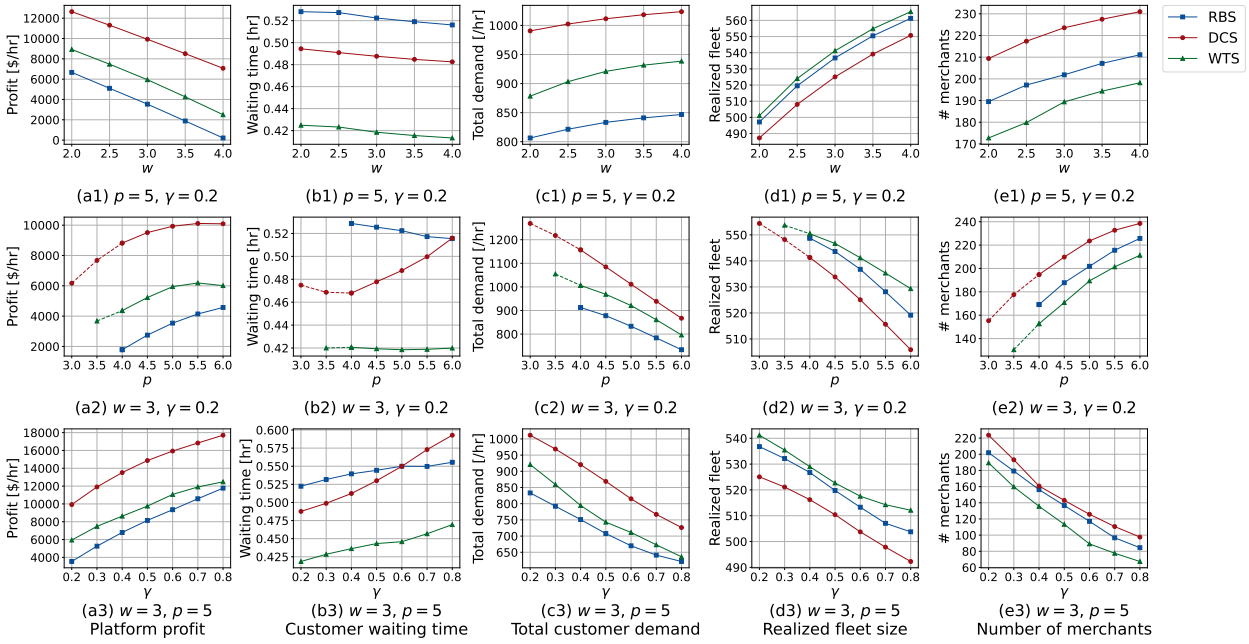

Figure 13: Impact of γ, w, and p on system metrics

However, if the wage is close to the delivery fee, the relationship of metrics may exhibit non-monotonic behaviors, e.g., Figure 13.b2, and under some conditions the equilibrium is not even reachable because of over-saturation of customers and thus delivery insufficiency. The platform intervention, especially DCS, exhibits again its superiority against ill demand–supply conditions. The third row of Figure 13 presents the impact of commission charge, a proportion of restaurants' revenue that is taken by the platform. Although its direct influence is only on the number of merchants willing to be online on the platform, it also endogenously impacts all other entities. As γ increases, the platform's profit is directly impacted, and it increases as well. However, less merchants will be willing to be online on the platform and in turn, affect the customer demand

and drivers' earnings. As γ increases, the customer waiting time under DCS surges more rapidly than that under RBS, indicating a negative impact of DCS under a high-commission market. We acknowledge that the behavior model of merchants could be further improved if empirical surveys could be delivered, but it lies outside the scope of this study. In our experiment, we interpret the major and direct impact of commission increase usually outpaces the impact from demand loss, which leads to a monotone-like trend of the profit curve. This could be a result of the three-sided equilibrium because all the other players are endogenously impacted by one player, while the commission is direct.

7 Conclusion

This paper introduces a network equilibrium model for the three-sided OFD system. The model can be applied to analyze the complex interplay among three market players, i.e., customers, drivers, and merchants, whose behaviors are affected by the operational decisions of the OFD platform. The delivery process is treated as a bundling dispatching problem where drivers are assigned to delivery paths. This approach enables us to jointly investigate the matching and bundling delivery as a whole and analyze the OFD market in stationary conditions. We showcase the model's ability to evaluate the performances of three different dispatching strategies, i.e., the random-bundling strategy (RBS), the delivery cost minimization strategy (DCS), and the waiting time minimization strategy (WTS), and discuss their properties and implications. This study extends the existing literature to model the OFD market as a three-sided market and derive network matching equilibrium.

Using the proposed model, we demonstrate its practical value by analyzing the flow patterns of delivery, pickup, and vacant drivers based on a real-world dataset. We compare and analyze the differences among the results of three delivery dispatching strategies. Our numerical studies reveal that, platform intervention (i.e., applying DCS or WTS) on the delivery dispatching process is beneficial in improving delivery supply, by assigning drivers to a few paths that utilize the delivery capacity. It also implies that bundling orders from different regions is only necessary when some regions are in short supply of delivery, which initiates inter-regional delivery to supplement the delivery supply. Results in numerical experiments also reveal that the platform's intervention in delivery dispatching enhances the overall system-wide performance by increasing platform profit and reducing customer waiting time. The proposed model has implications for governments and OFD platforms to plan appropriate managerial and operational strategies to improve the system's efficiency.

Our work provides a fundamental modeling framework for network analyses and optimization of on-demand food delivery services at a planning level. There are a few limitations to our research. Firstly, we acknowledge the possibility of reduced heterogeneity within regions due to the approximation of intra-regional travel time using a distribution. Investigating this effect may require a

more microscopic model to capture the vehicle routings of individual drivers. Second, we simplified the variations among merchants and orders, including the food product and consumer preferences, the variations in the demand–supply relationships, and the simplification of customer/driver attractiveness on target destinations only which neglects the influence of adjacent regions. Additionally, our model assumes that the decision of merchants to be online on the platform is short-term, based on their within-day online time. The behavior models of all three players could be calibrated by survey data and improved by more comprehensive behavior theories, while in this study, the existing data could not support the parameter calibration. Despite these limitations, the core focus of our model, which is the network-wise equilibrium, remains robust. This equilibrium is a reflection of the "average" behavior of each player. We view these limitations not as drawbacks but as avenues for further exploration in the field of OFD. Future research could be done on creating an operational decision model on a more microscopic level, and developing behavioral theories for market players (ideally based on a rich availability of data).

8 Acknowledgments

This work is supported by the Hong Kong Research Grants Council under Early Career Scheme Project No. HKU27203323 and the Hong Kong PhD Fellowship Scheme. Kaihang Zhang would like to thank the discussion with Dr. Anke Ye regarding the solution algorithm.

Declaration of generative AI and AI-assisted technologies

During the preparation of this work, the authors used generative AI tools to improve the language and readability of some parts of this work. After using this tool, the authors reviewed and edited the content as needed and took full responsibility for the content of the publication.

References

Alonso-Mora, J., Samaranayake, S., Wallar, A., Frazzoli, E., & Rus, D. (2017). On-demand high-capacity ride-sharing via dynamic trip-vehicle assignment. *Proceedings of the National Academy of Sciences*, *114*(3), 462–467.

Angrist, J. D., Caldwell, S., & Hall, J. V. (2021). Uber versus taxi: A driver's eye view. *American Economic Journal: Applied Economics*, *13*(3), 272–308.

Bahrami, S., Nourinejad, M., Nesheli, M. M., & Yin, Y. (2022). Optimal composition of solo and pool services for on-demand ride-hailing. *Transportation Research Part E: Logistics and Transportation Review*, *161*, 102680.

Bahrami, S., Nourinejad, M., Yin, Y., & Wang, H. (2023). The three-sided market of on-demand delivery. *Transportation Research Part E: Logistics and Transportation Review*, *179*, 103313.

Behrendt, A., Savelsbergh, M., & Wang, H. (2023). A prescriptive machine learning method for courier scheduling on crowdsourced delivery platforms. *Transportation Science*, *57*(4), 889–907.

Ben-Akiva, M. E., & Lerman, S. R. (1985). *Discrete choice analysis: Theory and application to travel demand* (Vol. 9). MIT press.

Berbeglia, G., Cordeau, J.-F., & Laporte, G. (2010). Dynamic pickup and delivery problems. *European Journal of Operational Research*, *202*(1), 8–15.

Boyd, S. P., & Vandenberghe, L. (2004). *Convex optimization*. Cambridge University Press.

Brouwer, L. E. J. (1911). Über abbildung von mannigfaltigkeiten. *Mathematische annalen*, *71*(1), 97–115.

Brualdi, R. A. (2010). *Introductory combinatorics (5th ed.)* Pearson Prentice Hall.

Castillo, J. C., Knoepfle, D., & Weyl, E. G. (2025). Matching and pricing in ride hailing: Wild goose chases and how to solve them. *Management Science*, *71*(5), 4377–4395.

Chen, M., Hu, M., & Wang, J. (2022). Food delivery service and restaurant: Friend or foe? *Management Science*, *68*(9), 6539–6551.

Chen, W., Yang, L., Chen, X., & Ke, J. (2025). Scaling laws of dynamic high-capacity ride-sharing. *Transportation Research Part C: Emerging Technologies*, *174*, 105064.

Chen, X., Zheng, H., Ke, J., & Yang, H. (2020). Dynamic optimization strategies for on-demand ride services platform: Surge pricing, commission rate, and incentives. *Transportation Research Part B: Methodological*, *138*, 23–45.

Courcoubetis, C., Li, Y., Gao, S., & Huang, Q. (2024). The impact of ride-hailing in city transportation. *Frontiers of Engineering Management*, *11*(4), 759–765.

Daganzo, C. F., & Ouyang, Y. (2019). *Public transportation systems: Principles of system design, operations planning and real-time control*. World Scientific.

Di, X., & Ban, X. J. (2019). A unified equilibrium framework of new shared mobility systems. *Transportation Research Part B: Methodological*, *129*, 50–78.

Dong, T., Luo, Q., Xu, Z., Yin, Y., & Wang, J. (2024). Strategic driver repositioning in ride-hailing networks with dual sourcing. *Transportation Research Part C: Emerging Technologies*, *158*, 104450.

Du, Z., Fan, Z.-P., & Chen, Z. (2023). Implications of on-time delivery service with compensation for an online food delivery platform and a restaurant. *International Journal of Production Economics*, *262*, 108896.

Guan, J., & Bao, Y. (2024). Does e-hailing perform better than on-street searching? an investigation based on the temporal-spatial distributions of idle vehicles. *Frontiers of Engineering Management*, *11*(4), 710–720.

He, F., & Shen, Z.-J. M. (2015). Modeling taxi services with smartphone-based e-hailing applications. *Transportation Research Part C: Emerging Technologies*, *58*, 93–106.

Hildebrandt, F. D., & Ulmer, M. W. (2022). Supervised learning for arrival time estimations in restaurant meal delivery. *Transportation Science*, *56*(4), 1058–1084.

Hu, X., Zhang, G., Shi, Y., & Yu, P. (2024). How information and communications technology affects the micro-location choices of stores on on-demand food delivery platforms: Evidence from xinjiekou's central business district in nanjing. *ISPRS International Journal of Geo-Information*, *13*(2), 44.

Indeed. (2025). Delivery driver hourly salaries in the united states at ubereats [Accessed: Apr 27, 2025]. https://www.indeed.com/cmp/Ubereats/salaries/Delivery-Driver

Ke, J., Wang, C., Li, X., Tian, Q., & Huang, H.-J. (2024). Equilibrium analysis for on-demand food delivery markets. *Transportation Research Part E: Logistics and Transportation Review*, *184*, 103467.

Ke, J., Yang, H., Li, X., Wang, H., & Ye, J. (2020a). Pricing and equilibrium in on-demand ride-pooling markets. *Transportation Research Part B: Methodological*, *139*, 411–431.

Ke, J., Yang, H., & Zheng, Z. (2020b). On ride-pooling and traffic congestion. *Transportation Research Part B: Methodological*, *142*, 213–231.

Konishi, H. (2005). Concentration of competing retail stores. *Journal of Urban economics*, *58*(3), 488–512.

Leonardi, M., & Moretti, E. (2023). The agglomeration of urban amenities: Evidence from milan restaurants. *American Economic Review: Insights*, *5*(2), 141–157.

Li, C., Mirosa, M., & Bremer, P. (2020). Review of online food delivery platforms and their impacts on sustainability. *Sustainability*, *12*(14), 5528.

Li, X., Ke, J., Yang, H., Wang, H., & Zhou, Y. (2024). An aggregate matching and pick-up model for mobility-on-demand services. *Transportation Research Part B: Methodological*, *190*, 103070.

Li, Y., & Phillips, W. (2018). *Learning from route plan deviation in last-mile delivery* (Master's dissertation). MIT. MA. https://dspace.mit.edu/bitstream/handle/1721.1/118135/Li_Phillips_2018_Capstone.pdf?sequence=1

Liang, J., Ke, J., Wang, H., Ye, H., & Tang, J. (2023). A poisson-based distribution learning framework for short-term prediction of food delivery demand ranges. *IEEE Transactions on Intelligent Transportation Systems*, 1–14.

Liang, J., Zhao, Y., Wang, H., Xiao, Z., & Ke, J. (2024). Uncovering merchants' willingness to wait in on-demand food delivery markets. *Transport Policy*, *158*, 14–28.

Little, J. D. C. (1961). A Proof for the Queuing Formula: $L = \lambda\ W$. *Operations Research*, *9*(3), 383–387.

Liu, J., Pei, S., & Zhang, X. (2023). Online food delivery platforms and female labor force participation. *Information Systems Research*, isre.2021.0182.

Liu, S., He, L., & Max Shen, Z.-J. (2021). On-time last-mile delivery: Order assignment with travel-time predictors. *Management Science*, *67*(7), 4095–4119.

Luo, Q., Nagarajan, V., Sundt, A., Yin, Y., Vincent, J., & Shahabi, M. (2023). Efficient algorithms for stochastic ride-pooling assignment with mixed fleets. *Transportation Science*, *57*(4), 1–29.

Lyu, G., Cheung, W. C., Teo, C.-P., & Wang, H. (2023). Multiobjective stochastic optimization: A case of real-time matching in ride-sourcing markets. *Manufacturing & Service Operations Management*, msom.2020.0247.

Mao, W., Ming, L., Rong, Y., Tang, C. S., & Zheng, H. (2019). Faster deliveries and smarter order assignments for an on-demand meal delivery platform. (ssrn. 3469015).

Mao, W., Ming, L., Rong, Y., Tang, C. S., & Zheng, H. (2022). On-demand meal delivery platforms: Operational level data and research opportunities. *Manufacturing & Service Operations Management*, *24*(5), 2535–2542.

Nguyen-Phuoc, D. Q., Nguyen, N. A. N., Nguyen, M. H., Nguyen, L. N. T., & Oviedo-Trespalacios, O. (2022). Factors influencing road safety compliance among food delivery riders: An extension of the job demands-resources (jd-r) model. *Transportation Research Part A: Policy and Practice*, *166*, 541–556.

Reyes, D., Erera, A., Savelsbergh, M., Sahasrabudhe, S., & O'Neil, R. (2018). The meal delivery routing problem. *Optimization online*, *6571*.

Simoni, M. D., & Winkenbach, M. (2023). Crowdsourced on-demand food delivery: An order batching and assignment algorithm. *Transportation Research Part C: Emerging Technologies*, *149*, 104055.

Sun, H., Wang, H., & Wan, Z. (2019). Model and analysis of labor supply for ride-sharing platforms in the presence of sample self-selection and endogeneity. *Transportation Research Part B: Methodological*, *125*, 76–93.

The Business Research Company. (2024). *Online food delivery services global market report 2024*. https://www.thebusinessresearchcompany.com/report/online-food-delivery-services-global-market-report

Train, K. E. (2009). *Discrete choice methods with simulation*. Cambridge university press.

Ulmer, M. W., Thomas, B. W., Campbell, A. M., & Woyak, N. (2021). The restaurant meal delivery problem: Dynamic pickup and delivery with deadlines and random ready times. *Transportation Science*, *55*(1), 75–100.

Wang, H. (2022). Transportation-enabled urban services: A brief discussion. *Multimodal Transportation*, *1*(2), 100007.

Wang, H., & Yang, H. (2019). Ridesourcing systems: A framework and review. *Transportation Research Part B: Methodological*, *129*, 122–155.

Wang, J., Wang, X., Yang, S., Yang, H., Zhang, X., & Gao, Z. (2021). Predicting the matching probability and the expected ride/shared distance for each dynamic ridepooling order: A

mathematical modeling approach. *Transportation Research Part B: Methodological*, *154*, 125–146.

Wang, X., Agatz, N., & Erera, A. (2018). Stable matching for dynamic ride-sharing systems. *Transportation Science*, *52*(4), 850–867.

Wardrop, J. G. (1952). Some theoretical aspects of road traffic research. *Proceedings of the Institution of Civil Engineers*, *1*(3), 325–362.

Wright, S. J. (2015). Coordinate descent algorithms. (arXiv:1502.04759). http://arxiv.org/abs/1502.04759

Xu, Z., Chen, Z., Yin, Y., & Ye, J. (2021). Equilibrium analysis of urban traffic networks with ride-sourcing services. *Transportation Science*, *55*(6), 1260–1279.

Yang, H., Leung, C. W., Wong, S., & Bell, M. G. (2010). Equilibria of bilateral taxi–customer searching and meeting on networks. *Transportation Research Part B: Methodological*, *44*(8–9), 1067–1083.

Yang, H., Qin, X., Ke, J., & Ye, J. (2020). Optimizing matching time interval and matching radius in on-demand ride-sourcing markets. *Transportation Research Part B: Methodological*, *131*, 84–105.

Yang, H., & Wong, S. (1998). A network model of urban taxi services. *Transportation Research Part B: Methodological*, *32*(4), 235–246.

Ye, A., Zhang, K., Bell, M. G., Chen, X., & Hu, S. (2024a). Modeling an on-demand meal delivery system with human couriers and autonomous vehicles in a spatial market. *Transportation Research Part C: Emerging Technologies*, 104723.

Ye, A., Zhang, K., Chen, X., Bell, M. G., Lee, D.-H., & Hu, S. (2024b). Modeling and managing an on-demand meal delivery system with order bundling. *Transportation Research Part E: Logistics and Transportation Review*, *187*, 103597.

Yildiz, B., & Savelsbergh, M. (2019). Service and capacity planning in crowd-sourced delivery. *Transportation Research Part C: Emerging Technologies*, *100*, 177–199.

Zhang, K., Ke, J., Wang, H., & Yin, Y. (2025). Tactical operations of service region dimensioning, bundling, and matching for on-demand food delivery services. *Transportation Research Part C: Emerging Technologies*, *174*, 105069.

Zhang, K., Mittal, A., Djavadian, S., Twumasi-Boakye, R., & Nie, Y. (2023). Ride-hail vehicle routing (river) as a congestion game. *Transportation Research Part B: Methodological*, *177*, 102819.

Zhang, K., & Nie, Y. (2021). To pool or not to pool: Equilibrium, pricing and regulation. *Transportation Research Part B: Methodological*, *151*, 59–90.

Zhu, L., Yu, W., Zhou, K., Wang, X., Feng, W., Wang, P., Chen, N., & Lee, P. (2020). Order fulfillment cycle time estimation for on-demand food delivery. *Proceedings of the 26th ACM SIGKDD International Conference on Knowledge Discovery & Data Mining*, 2571–2580.

Appendix A Notation

The following notation conventions are used in this paper. The term "be defined as" is written as :=. Scalars are written in unbolded letters. Sets are written in calligraphic capital letters, $\mathcal{N}$, for instance. For any set $\mathcal{S}$, $|\mathcal{S}|$ denotes the cardinality, i.e., the number of elements in this set unless otherwise specified. The lowercase letters on the subscript position mean the locational information while those on the superscript position mean the symbol's attributes such as "v" denoting for "vacant drivers", etc. We use bolded lowercase letters such as $\mathbf{v}$ to denote vectors and bolded capital letters to denote matrices such as $\mathbf{M}$.

Table 4: Basic notation and definitions

Variables	Definition	Vector form
Decision variables		
$\lambda^o_{m,i}$	The vehicular flow of occupied drivers serving the i^{th} bundle of the merchant at $m \in \mathcal{N}^{\text{mer}}$ $(i \in \mathcal{I}_m)$	$\boldsymbol{\lambda}^o_{\mathcal{P}}$
λ^{μ}_{vm}	The matching rate of drivers at v to m	$\boldsymbol{\lambda}^{\mu}$
Equilibrium variables		
m^{cus}_m	The number of customers' order bundles in merchants at nodal location $m \in \mathcal{N}^{\text{mer}}$	$\mathbf{m}^c$
m^{dr}_v	The number of awaiting drivers (vehicles) at nodal location $v \in \mathcal{N}^{\text{dr}}$	$\mathbf{m}^v$
m^{mer}_m	The number of merchants that are willing to be online on the platform at $m \in \mathcal{N}^{\text{mer}}$	$\mathbf{m}^m$
Sets		
$\mathcal{N}$	Complete set of all nodal locations	
$\mathcal{N}^{\text{cus}} \subseteq \mathcal{N}$	Set of customer nodal locations	
$\mathcal{N}^{\text{mer}} \subseteq \mathcal{N}$	Set of merchant (restaurant) nodal locations	
$\mathcal{N}^{\text{dr}} \subseteq \mathcal{N}$	Set of vacant driver nodal locations	
$\mathcal{N}^{\text{del}}_m \subseteq \mathcal{N}$	Set of nodal locations within the delivery area of the merchant at $m \in \mathcal{N}^{\text{mer}}$	
$\mathcal{N}^{\text{match}}_m \subseteq \mathcal{N}$	Set of nodal locations within the matching area of the merchant at $m \in \mathcal{N}^{\text{mer}}$	
B^k_m	A possible order bundle of size k of merchants at $m \in \mathcal{N}^{\text{mer}}$	
$\mathcal{B}^k_m$	Set of all possible order bundles of size k from merchant at $m \in \mathcal{N}^{\text{mer}}$	
$\mathcal{B}_m$	Set of all possible order bundles from merchant at $m \in \mathcal{N}^{\text{mer}}$, $\mathcal{B}_m \supset \mathcal{B}^k_m$ for $k \leq \hat{k}$	
$\mathcal{B}_{m,i} \in \mathcal{B}_m$	The i^{th} bundle of merchants at $m \in \mathcal{N}^{\text{mer}}$ $(i \in \mathcal{I}_m)$	
$\mathcal{I}_m$	Set of indexes of order bundles corresponding to the merchant at $m \in \mathcal{N}^{\text{mer}}$	

Page over

Table 4: Basic notation and definitions continued

Variables	Definition	Vector form
$\mathcal{P}_m$	Set of all the sequences of the order bundles $\mathcal{B}_m$ (see Definition 2) of the merchant at $m \in \mathcal{N}^{\text{mer}}$	
$\mathcal{P}_{m,i} \in \mathcal{P}_m$	The shortest path corresponding to $\mathcal{B}_{m,i}$.	
$\mathcal{S}_e$	Solution set of m_m^{cus}, m_v^{dr}, and m_m^{mer} defined by the three-sided equilibrium	
$\mathcal{F}_\mu$	Feasible set of the matching flow	
$\mathcal{F}_d$	Feasible set of the delivery path flow	
Functions		
$C(c, \mathcal{B}_{m,i})$	The count of customers c in bundle $\mathcal{B}_{m,i}$	
$\text{Pm}(\mathcal{S})$	All the permutations of set $\mathcal{S}$	
$\text{Unique}(\mathcal{S})$	The unique items in set $\mathcal{S}$	
$\lvert\cdot\rvert_p$	The number of unique permutations of set $\mathcal{S}$	
Exogenous variables		
p	Delivery fee per distance	
p_o	Average order price for each order	
w	Wage paid to drivers per distance	
γ	Commission charged to merchants as a proportion of revenue	
β	Value of time	
τ	Batch-matching time interval	
t_s	Drivers' dwell time after completing the delivery of an order	
k	Number of orders in each bundle	
$\hat{k}$	Bundling capacity	
$\hat{m}_m^{\text{mer}}$	Total number of restaurants in the region $m \in \mathcal{N}^{\text{mer}}$	
$\hat{N}_F$	Vehicle fleet size	
$A_{c,m}^{\text{cus}}$	Attractiveness of merchants at $m \in \mathcal{N}^{\text{mer}}$ to customers at $c \in \mathcal{N}^{\text{cus}}$	
A_{cv}^{dr}	Attractiveness of each region $v \in \mathcal{N}^{\text{dr}}$ to vacant drivers who completed their preceding delivery task at $c \in \mathcal{N}^{\text{cus}}$	
$d_{m,i}$	The shortest-path distance starting from the merchant at $m \in \mathcal{N}^{\text{mer}}$ and visiting all customers in the order bundle $\mathcal{B}_{m,i}$	$\mathbf{d}$
L_{xy}	Distance from nodal location x to nodal location y, $(x,y) \in \{(c,v),(v,m),(c,m)\}$	$\mathbf{l}_{xy}$
Intermediate variables		
$q_{c,m}$	The demand rate of customers from c to merchant $m \in \mathcal{N}^{\text{mer}}$	$\mathbf{q}$
$W_{m,i}^a$	The accumulation time induced by each order bundle	$\mathbf{w}_a(\mathbf{q})$
λ_{mc}^{OT}	The OT flow of the food delivery supply from $m \in \mathcal{N}^{\text{mer}}$ through c	$\boldsymbol{\lambda}^o$
λ_{cv}^{φ}	The vehicular flow of vacant drivers traveling from $c \in \mathcal{N}^{\text{cus}}$ to $v \in \mathcal{N}^{\text{dr}}$	$\boldsymbol{\lambda}^{\varphi}$

Page over

Table 4: Basic notation and definitions continued

Variables	Definition	Vector form
λ_{vm}^{p}	The vehicular flow of drivers in a pickup journey traveling from $v \in \mathcal{N}^{\mathrm{dr}}$ to $m \in \mathcal{N}^{\mathrm{mer}}$	$\boldsymbol{\lambda}^{p}$
$V_{c,m}^{\mathrm{cus}}$	General monetary utility of customers from node c to select merchants at node m	
$U_{c,m}^{\mathrm{cus}}$	Random utility considering perception error of $V_{c,m}^{\mathrm{cus}}$	
V_{cv}^{dr}	General monetary utility of vacant drivers traveling from node $c \in \mathcal{N}^{\mathrm{cus}}$ to node $v \in \mathcal{N}^{\mathrm{dr}}$	
U_{cv}^{dr}	Random utility considering perception error of V_{cv}^{dr}	
$\check{F}_v$	The expected earning for vacant drivers moving to node $v \in \mathcal{N}^{\mathrm{dr}}$	
$\check{h}_v$	The expected service time for vacant drivers moving to node $v \in \mathcal{N}^{\mathrm{dr}}$	
$\bar{F}_m$	The average earning for occupied drivers serving merchants at node $m \in \mathcal{N}^{\mathrm{mer}}$	
$\bar{h}_m$	The average delivery time for occupied drivers serving merchants at node $m \in \mathcal{N}^{\mathrm{mer}}$	
N_F	Realized vehicle fleet size	
W_m^{cus}	Average waiting time of customers for selecting merchant at $m \in \mathcal{N}^{\mathrm{mer}}$	
W_v^{dr}	Average waiting time of drivers for selecting waiting location at $v \in \mathcal{N}^{\mathrm{dr}}$	
Initialism		
BDD	Bundling delivery dispatching	
BM	Batch-matching	
MPEC	Mathematical program with equilibrium constraints	
OFD	On-demand food delivery	
RS	Ride-sourcing	
RBS	random-bundling strategy	
DCS	Delivery cost minimization strategy	
WTS	Waiting time minimization strategy	

Appendix B Sources of stochasticity in the model

B.1 Intra-regional distance

The inter-regional distance in this study is approximated to be the geographical distance between two nodes. We neglect the uncertainties associated with traffic or locational stochasticity, following the modeling prototypes of existing studies, e.g., He and Shen (2015) and Ye et al. (2024a), respectively. For intra-regional travel, we use the following procedure to approximate the average distance using an *approximated circle*. We borrow the idea from the literature (e.g., Yang et al., 2020 and Li et al., 2024) to represent the catchment area of a merchant node using the idea called

dominant zone, see Figure 14 as an illustration. If we treat half of the distance from a node to each of its adjacent nodes as the radius of a surrounding circle (black circles in Figure 14) and there are multiple of these circles. In the figure, the red dots denote empirical centroids representing each region where merchant clusters may be located. We approximate the dominant zone of a merchant region using the average of surrounding circles and thus results in an average circle with radius r_m, m standing for the index of a merchant region. Since the distance between two nodes is twice of the radius of a surrounding circle, r_m is the average of the sum of the distances to its adjacent nodes and divided by 2, i.e., $r_m = \frac{1}{2}\sum_n d_{m,n}$ where n denotes the adjacent nodes (in Figure 14, they are $\{2,3,4,5\}$) and $d_{m,n}$ denote the distance from merchant m to merchant n. Finally, if we assume a homogeneous distribution of customers in each region, and with a well-known result that the expected distance from the center of a circle to a random point within a circle is 2/3 of its radius, the expected intra-nodal distance is empirically $d_m = \frac{2}{3}r_m = \frac{1}{3}\sum_n d_{m,n}$. By using this approximation, we eliminate the 0 distance of intra-nodal delivery, which is unrealistic and also helps regularize our calculation. This approximation is mostly accurate when the partitioning of a region results in fine-grained areas. In other words, it is useful when areas are small. However, applying deterministic distance to a random point may lead to inaccuracy, especially when the dominant zone of a merchant node is not sufficiently small. But the model can be easily implemented to stochastic programming if needed by introducing a random error to the distance, $\tilde{\xi}^d_m$. Then we have $\tilde{d}_m = d_m + \tilde{\xi}^d_m$. The stochastic intra-regional distance can be implemented using random sampling–based simulation in the calculation process (Train, 2009, pp233–269), also known as the sample average approximation (SAA) in stochastic programming. We solve for the problem in a stochastic setting in Appendix B.4, but maintain the deterministic approximation in our model to provide a foundation for future extensions.

B.2 Customer attractiveness

We adopt a relationship with decreasing marginal utility gain from an increasing number of merchants, in the form of $[1-\exp(-\theta^{\text{cus},a} m_m^{\text{mer}})]\cdot \hat{A}^{\text{cus}}_{c,m}$ for illustration purposes, where m_m^{mer} denotes the number of merchants at m, $\theta^{\text{cus},a}$ and $\hat{A}^{\text{cus}}_{c,m}$ are coefficients. The multiplier to $\hat{A}^{\text{cus}}_{c,m}$ can be seen as a coefficient ranging from 0 to 1 to scale the attractiveness depending on the number of merchants.

The constant $\hat{A}^{\text{cus}}_{c,m}$ is essentially an alternative-specific coefficient in the model because it varies across customers and merchants. The consideration of "attractiveness" is useful in a few aspects. First, the attractiveness term has the ability to capture the latent influences such as the price of meals and their quality. Second, the alternative-specific coefficient makes it more flexible to capture real-world spatial heterogeneity because customer preferences may exhibit differences across space. Nonetheless, this behavioral model is for illustrative purposes because practitioners can easily switch to other models if necessary, such as linear, or replacing $\theta^{\text{cus},a}$ with an alternative-specific

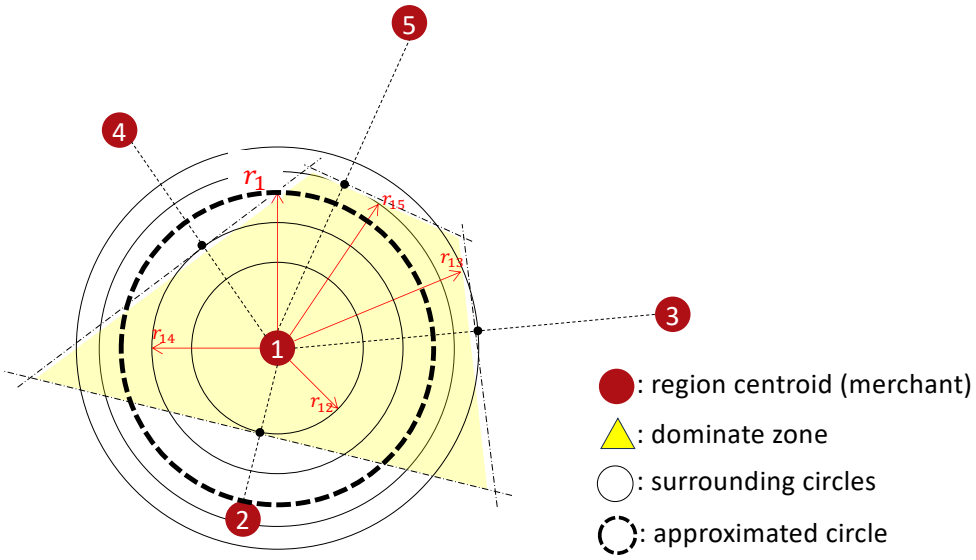

Figure 14: Illustration of the surrounding circle approximation

coefficient if necessary to capture people's heterogeneous attitudes toward the number of merchants in each region. However, it is worth mentioning that our model is based upon the assumption that merchants produce homogeneous products, and they can be represented by the average attributes (e.g., delivery time, matching time, etc.) of merchants in that region. Considering the randomness of the attractiveness of merchants in each region, the attractiveness $\hat{A}^{\text{cus}}_{c,m}$ is subject to uncertainty. Similar to our discussion regarding intra-nodal distance, we can treat $\hat{A}^{\text{cus}}_{c,m}$ as a random variable, which has the ability to capture the uncertainty of customers' preference of restaurants in a region, see our demonstration of a stochastic program in Appendix B.4. In terms of calibration process, the coefficients $\theta^{\text{cus},a}$ and θ^{cus} as well as the alternative-specific coefficient $\hat{A}^{\text{cus}}_{c,m}$ can be calibrated using real-world survey data, e.g., perform stated-preference surveys and fit the data using maximum likelihood estimation or simulation-based methods for parameter estimation (Train, 2009, pp41–85). For example, stated-preference surveys can be designed to ask people which merchant they would prefer when several merchants are provided for them to choose, where each merchant has different attributes (number of merchants surrounding, distance, average delivery time, etc.). Calibrating such models may require a sufficient number of survey responses from customers who make statements of which merchants they would prefer, given a few alternatives. The merchant-related data are also not difficult to obtain, such as the number of restaurants in each region, etc.

B.3 Driver attractiveness

If we consider a form of A_{cv}^{dr} similar with that of customer demand, we have $A_{cv}^{\mathrm{dr}} = [1 - \exp(-\theta^{\mathrm{dr},a} m_v^m)] \cdot \hat{A}_{cv}^{\mathrm{dr}}$ where m_v^m denotes the number of merchants willing to be online on the platform at v, $\theta^{\mathrm{dr},a}$ and $\hat{A}_{cv}^{\mathrm{dr}}$ the coefficients for the choice model. Similar to the choice model of customers, $\hat{A}_{cv}^{\mathrm{dr}}$ can be seen as an alternative specific coefficient representing the spatial heterogeneity of drivers' attitudes across regions. We also present the demo of considering stochastic attractiveness in Appendix B.4. These parameters as well as θ^{dr} can be calibrated by conducting stated preference surveys and doing parameter estimation.

B.4 A stochastic program illustration

We discuss in this section regarding the randomness involved in our model. From Sections 3 and 4.1, we consider three sources of randomness in this section, namely the intra-nodal travel distance, attractiveness of merchants to customers, and attractiveness of each location to vacant drivers. We denote their random terms as $\tilde{\boldsymbol{\xi}}^d$, $\tilde{\boldsymbol{\xi}}^c$, and $\tilde{\boldsymbol{\xi}}^v$, respectively, and stack them into a unified vector $\tilde{\boldsymbol{\xi}}$. For illustration purposes, we use the Gaussian distribution with 0 mean and a small standard deviation that almost prevents drawing negative values (for instance, for intra-nodal distance, the standard deviation is taken to be $1/4$ of d_m for each merchant). Since these are from different players and have different sources of randomness, we can assume that these random variables are i.i.d.. Following the structure of the stochastic programming in Boyd and Vandenberghe (2004, pp. 209), we take the expectation of the objective functions and constraints to consider the problem under an expected scenario with respect to the uncertainties in intra-nodal traveling. Then, from Equations (1) and (23), the SMD problem becomes

[SMD-SP] : (41a)

$$\min_{\mathbf{m},\boldsymbol{\lambda}^{\mu},\boldsymbol{\lambda}^{o}_{\mathcal{P}}} \quad \mathbb{E}\left[f_{\mu}(\mathbf{m},\boldsymbol{\lambda}^{\mu},\tilde{\boldsymbol{\xi}}) + f_{d}(\mathbf{q},\boldsymbol{\lambda}^{o}_{\mathcal{P}},\tilde{\boldsymbol{\xi}})\right] \tag{41b}$$

$$\text{s.t.} \quad \mathbb{E}(h_1) = \mathbb{E}\left[\mathbf{q} - g(\mathbf{m},\boldsymbol{\lambda}^{\mu},h(\mathbf{q}),\tilde{\boldsymbol{\xi}})\right] = 0, \tag{41c}$$

$$\mathbb{E}(h_2) = \mathbb{E}\left[\sum_{m}\lambda^{\mu}_{vm} - \sum_{c}\lambda^{\varphi}_{cv}(\mathbf{m},\boldsymbol{\lambda}^{\mu},\boldsymbol{\lambda}^{o}_{\mathcal{P}},\tilde{\boldsymbol{\xi}})\right] = 0, \tag{41d}$$

$$\mathbb{E}(h_3) = \mathbb{E}\left[\sum_{v\in\mathcal{N}^{\text{match}}_{m}}\lambda^{\mu}_{vm} - \sum_{i\in\mathcal{I}_m}\lambda^{o}_{m,i}\right] = 0, \tag{41e}$$

$$\mathbb{E}(h_4) = \mathbb{E}\left[N_F - \sum_{m}\sum_{i\in\mathcal{I}_m}h_{m,i}\lambda^{o}_{m,i} + \sum_{c}\sum_{v}h_{cv}\lambda^{\varphi}_{cv}(\mathbf{m},\boldsymbol{\lambda}^{\mu},\boldsymbol{\lambda}^{o}_{\mathcal{P}},\tilde{\boldsymbol{\xi}}) + \sum_{m}\sum_{v}h_{vm}\lambda^{\mu}_{vm} + \sum_{v}m^{\text{dr}}_{v}\right] = 0, \tag{41f}$$

$$\mathbb{E}(h_5) : \boldsymbol{\lambda}^{o}_{\mathcal{P}} \in \mathcal{F}_d := \left\{\boldsymbol{\lambda}^{o}_{\mathcal{P}} \,\middle|\, \mathbb{E}\left[\mathbf{A}(\tilde{\boldsymbol{\xi}})\boldsymbol{\lambda}^{o}_{\mathcal{P}} - \mathbf{q}\right] = 0\right\}, \tag{41g}$$

$$\boldsymbol{\lambda}^{\mu} \in \mathcal{F}_{\mu}(\mathbf{m}), \tag{41h}$$

[SMD-SP-SAA] : (42a)

$$\min_{\mathbf{q},\mathbf{m},\boldsymbol{\lambda}^{\mu},\boldsymbol{\lambda}^{o}_{\mathcal{P}}} \quad \frac{1}{N}\left[\sum_{n} f_{\mu}(\mathbf{q},\boldsymbol{\lambda}^{\mu},\boldsymbol{\xi}_n) + \sum_{n} f_{d}(\mathbf{q},\boldsymbol{\lambda}^{o}_{\mathcal{P}},\boldsymbol{\xi}_n)\right] \tag{42b}$$

$$\text{s.t.} \quad \frac{1}{N}\sum_{n}\mathbf{h}(\boldsymbol{\xi}_n) = 0, \tag{42c}$$

$$\boldsymbol{\lambda}^{\mu} \in \mathcal{F}_{\mu}(\mathbf{m}), \tag{42d}$$

where $\mathbf{h}$ represents the vector for all equality constraint functions. If we choose $N = 100$, and the settings $\hat{k} = 4$, $\hat{N}_F = 600$, and all default pricing settings as stated in Section 6.5 we have the following metrics.

Appendix C Proof of Claim 1

To prove that the transformations from $\boldsymbol{\lambda}^{o}_{\mathcal{P}}$ to $W^{cd}_{c,m}$ and W^{cd} are linear, we just need to construct such transformations. We first construct a matrix $\mathbf{M}^{cd}$ ($|\mathcal{N}^{\text{cus}}|$ by $\sum_m I_m$) using the logic as follows. For each column (corresponding to each delivery path), the element (corresponding to each customer location) is assigned the delivery time if the corresponding path traverses this customer, and 0

Table 5: Metrics under each delivery dispatching strategy.

Metrics \ Strategies	RBS	DCS	WTS
Customer waiting time [hr]	0.51	0.49	0.41
Platform profit [$/hr]	4021	9113	6812
Total customer demand [/hr]	893.0	1040.2	1005.4
Total number of merchants	230.7	244.2	221.8
Realized vehicle fleet	543	542	549
Driver hourly earnings [$/hr]	22.5	22.2	23.7
Average bundling ratio	1.92	3.60	2.10

otherwise, where the delivery time is computed from the time that a driver leaves the restaurant to the time that the order is delivered to the customer at c, following the sequence specified in that path. Then, the average delivery time is computed as the average of the delivery times weighted by path flow

$$W^{cd} = \frac{\mathbf{1}^\top \mathbf{M}^{cd} \boldsymbol{\lambda}^o_{\mathcal{P}}}{\mathbf{k}^\top \boldsymbol{\lambda}^o_{\mathcal{P}}} = \frac{\mathbf{1}^\top \mathbf{M}^{cd}}{\mathbf{1}^\top \mathbf{q}} \boldsymbol{\lambda}^o_{\mathcal{P}}. \tag{43}$$

With $\mathbf{M}^{cd}$, we should notice that $\mathbf{M}^{cd}$ is a matrix that consists of $\mathbf{M}^{cd}_m$, i.e., $\mathbf{M}^{cd} := \begin{bmatrix} \mathbf{M}^{cd}_1 & \mathbf{M}^{cd}_2 & \dots & \mathbf{M}^{cd}_{|\mathcal{N}_m|} \end{bmatrix}$. We construct $\mathbf{M}^{cds}$ ($|\mathcal{N}^{\text{cus}}| \cdot |\mathcal{N}^{\text{mer}}|$ by $\sum_m I_m$):

$$\mathbf{M}^{cds} = \begin{bmatrix} \mathbf{M}^{cd}_1 & \mathbf{0} & \dots & \mathbf{0} \\ \mathbf{0} & \mathbf{M}^{cd}_2 & \dots & \mathbf{0} \\ \vdots & \vdots & \ddots & \vdots \\ \mathbf{0} & \mathbf{0} & \dots & \mathbf{M}^{cd}_m \end{bmatrix}. \tag{44}$$

Let $W^{cd}_{m,i,c}$ be the delivery time for customer c in bundle i of merchant m. The average delivery time for customers at c ordering food from merchant at m in Equation (2) is computed as

$$W^{cd}_{c,m} = \frac{\sum_{i \in \mathcal{I}_m} W^{cd}_{m,i,c} \lambda^o_{m,i}}{\sum_{i \in \mathcal{I}_m} \lambda^o_{m,i}} \tag{45}$$

$$= \mathbb{1}^\top_{c,m} (\mathbf{M}^{cds} \boldsymbol{\lambda}^o_{\mathcal{P}} \oslash \mathbf{q}), \tag{46}$$

where $\oslash$ denotes the element-wise division and $\mathbb{1}_{c,m}$ is an indicator vector of size cm by 1 and with value 1 at location $(m-1)|\mathcal{N}_c| + c$ and 0 elsewhere.

Appendix D Proof of Claim 2

Given a stacked vector for all the path flows of all merchants as $\boldsymbol{\lambda}^o_{\mathcal{P}}$, we construct a matrix in this proof such that

$$\mathbf{M}^{ce}\boldsymbol{\lambda}^o_{\mathcal{P}} = \boldsymbol{\lambda}^o_c = \left\{ \sum_m \sum_{\substack{i \text{ that } \mathcal{P}_{m,i} \\ \text{ended at } c}} \lambda^o_{m,i}, c \in \mathcal{N}^{\text{cus}} \right\}. \tag{47}$$

The matrix $\mathbf{M}^{ce}$ has shape $[|\mathcal{N}^{\text{cus}}|, \sum_m I_m]$ where $|\cdot|$ denotes cardinality. It is constructed as follows: for each merchant there is a submatrix, for each column (representing each delivery path of that merchant) of each submatrix, the index is assigned 1 if the corresponding customer node c is at the end of that path and 0 otherwise. Therefore,

$$\mathbf{M}^{ce} = \begin{bmatrix} \mathbf{M}^{ce,}_1 & \mathbf{M}^{ce}_2 & \dots & \mathbf{M}^{ce}_m \end{bmatrix}, \tag{48}$$

where, for instance,

$$\mathbf{M}^{ce}_m = \overbrace{\begin{bmatrix} 0 & 0 & \cdots & 0 \\ 0 & 0 & \cdots & 1 \\ 1 & 0 & \cdots & 0 \\ \vdots & \vdots & \ddots & \vdots \\ 0 & 1 & \cdots & 0 \end{bmatrix}}^{I_m \text{ columns}} \Bigg\} c \text{ rows.} \tag{49}$$

In the above example of merchant m, the first delivery path, indicated by the first column, has an end point at node 3, the second path at node c, and the last path at node 2.

If we do $\mathbf{M}^{ce}\boldsymbol{\lambda}^o_{\mathcal{P}}$, we obtain the sum of all flows that end at each node, realizing Equation (11).

Appendix E Proof of Claim 3

Before we proceed, we first claim two lemmas.

Lemma 1. *The second equality of Equation (20)*

$$\sum_{i \in \mathcal{I}_m} \lambda^o_{m,i} = \lambda_m \tag{50}$$

can be vectorized to

$$\mathbf{M}^{mp}\boldsymbol{\lambda}^o_{\mathcal{P}} = \boldsymbol{\lambda}^o_m \tag{51}$$

using a matrix $\mathbf{M}^{mp}$.

Proof. We construct such a matrix $\mathbf{M}^{mp}$ in this proof. It has shape $[m, \sum_m I_m]$ and it is constructed as follows: for each merchant (each row), the element is assigned 1 if the index corresponds to that merchant, and 0 otherwise. Therefore,

$$\mathbf{M}^{mp} = \begin{bmatrix} \mathbf{1}^\top_{I_1} & \mathbf{0}^\top_{I_2} & \mathbf{0}^\top_{I_3} & \dots & \mathbf{0}^\top_{I_m} \\ \mathbf{0}^\top_{I_1} & \mathbf{1}^\top_{I_2} & \mathbf{0}^\top_{I_3} & \dots & \mathbf{0}^\top_{I_m} \\ \mathbf{0}^\top_{I_1} & \mathbf{0}^\top_{I_2} & \mathbf{1}^\top_{I_3} & \dots & \mathbf{0}^\top_{I_m} \\ \vdots & \vdots & \vdots & \ddots & \vdots \\ \mathbf{0}^\top_{I_1} & \mathbf{0}^\top_{I_2} & \mathbf{0}^\top_{I_3} & \dots & \mathbf{0}^\top_{I_m} \\ \mathbf{0}^\top_{I_1} & \mathbf{0}^\top_{I_2} & \mathbf{0}^\top_{I_3} & \dots & \mathbf{1}^\top_{I_m} \end{bmatrix}, \tag{52}$$

where $\mathbf{1}^\top_{I_m}$ denotes a row vector of ones with length I_m and so does $\mathbf{0}^\top_{I_m}$. Loosely speaking, it also means that these locations correspond to the paths of the merchant indexed m. With $\mathbf{M}^{mp}$ constructed, we have $\mathbf{M}^{mp}\boldsymbol{\lambda}^o_{\mathcal{P}} = \boldsymbol{\lambda}^o_m$. ■

Lemma 2. *The calculation*

$$\sum_m \sum_{i \text{ that through } c} \lambda^o_{m,i} = \lambda^o_c \tag{53}$$

can be vectorized to

$$\mathbf{M}^{cc}\boldsymbol{\lambda}^o_{\mathcal{P}} = \boldsymbol{\lambda}^o_{throuth\ c} \tag{54}$$

using a matrix $\mathbf{M}^{cc}$.

Proof. We construct such a matrix $\mathbf{M}^{cc}$ in this proof. It has shape $[c, \sum_m I_m]$ and it is constructed similar to $\mathbf{M}^{ce}$ as follows: for each merchant there is a submatrix; for each column (representing each path of that merchant) of each submatrix, the index where the corresponding node is visited by that path is assigned 1, and 0 otherwise. Therefore,

$$\mathbf{M}^{cc} = \begin{bmatrix} \mathbf{M}^{cc}_1 & \mathbf{M}^{cc}_2 & \cdots & \mathbf{M}^{cc}_m \end{bmatrix} \tag{55}$$

where

$$\mathbf{M}_m^{cc} = \overbrace{\begin{bmatrix} 0 & 2 & \cdots & 0 \\ 1 & 0 & \cdots & 1 \\ 1 & 0 & \cdots & 1 \\ \vdots & \vdots & \ddots & \vdots \\ 0 & 1 & \cdots & 1 \end{bmatrix}}^{I_m \text{ columns}} \Bigg\} c \text{ rows.} \tag{56}$$

In the above example of merchant m, the first delivery path, represented by the first column, visits nodes 2, 3; the second path visits nodes 1 twice and c; and the last path visits nodes 2, 3, c.

If we do $\mathbf{M}^{cc}\boldsymbol{\lambda}_{\mathcal{P}}^{o}$, we obtain the sum of all flows that visits each node and thus we obtain the aggregate flow covering each node, or the total served demand from each customer location. ■

Given matrices $\mathbf{M}^{mp}$ and $\mathbf{M}^{cc}$, $\mathbf{A}$ and $\mathbf{b}$ are used for $\mathbf{A}\boldsymbol{\lambda}_{\mathcal{P}}^{o} = \mathbf{b}$ in linear programming constraints, representing demand–supply equilibrium. The construction of $\mathbf{A}$ follows these steps. First, we introduce $\mathbf{A}_m$:

$$c \text{ rows} \left\{ \begin{bmatrix} \mathbf{M}^{mp}[m,:] \\ \mathbf{M}^{mp}[m,:] \\ \vdots \\ \mathbf{M}^{mp}[m,:] \end{bmatrix} \right. \odot \mathbf{M}^{cc}, \tag{57}$$

where $\odot$ denotes element-wise product, $\mathbf{M}^{mp}[m,:]$ means the m-th row of $\mathbf{M}^{mp}$. Each $\mathbf{A}_m$ transforms the served demand of each merchant m for each customer location at c because the first item on the above equation filters $\mathbf{M}^{cc}$ to function for columns of only merchant m. Then, we let

$$\mathbf{A} = \begin{bmatrix} \mathbf{A}_1 \\ \mathbf{A}_2 \\ \cdots \\ \mathbf{A}_m \end{bmatrix} \Bigg\} c \cdot m \text{ rows,} \tag{58}$$

which transforms $\boldsymbol{\lambda}_{\mathcal{P}}^{o}$ to the served demand for each OD.

On the other hand, the actual demand $\mathbf{b}$ is computed as follows. Given demand matrix

$\mathbf{Q} := \{q_{c,m}\}$ and each column denoted as $\mathbf{q}_m$, we have

$$\mathbf{b} = \begin{bmatrix} \mathbf{q}_1 \\ \mathbf{q}_2 \\ \cdots \\ \mathbf{q}_m \end{bmatrix} \Bigg\} c \cdot m \text{ rows.} \tag{59}$$

With $\mathbf{A}$ and $\mathbf{b}$ defined, Equation (15) can be vectorized to $\mathbf{A}\boldsymbol{\lambda}^o_{\mathcal{P}} = \mathbf{q}$.

Appendix F Proof of the existence of the equilibrium

According to Yang et al. (2010) which investigate the network matching equilibrium of the taxi market, it suffices to prove the existence of the matching equilibrium by proving the existence of the fixed point system, i.e., there exists a pair of equilibrium variables such that $(\mathbf{m}^c, \mathbf{m}^v) \in \Gamma(\mathbf{m}^c, \mathbf{m}^v)$. We exclude $\mathbf{m}^m$ here because it can be obtained by the closed-form formula in Equation (14) which contains $\mathbf{m}^c$.

The existence of a fixed point system can be proved by using Brouwer's fixed point theorem (Brouwer, 1911). Let $\mathcal{M}$ be the feasible sets of the equilibrium state variables $\mathbf{m}^c$ and $\mathbf{m}^v$. According to Brouwer's fixed point theorem, if the mapping $\Gamma : \mathcal{M} \to \mathcal{M}$ is continuous, and $\mathcal{M}$ is compact and convex, there exists a fixed point of $(\mathbf{m}^c, \mathbf{m}^v) \in \mathcal{M}$ such that $(\mathbf{m}^c, \mathbf{m}^v) \in \Gamma(\mathbf{m}^c, \mathbf{m}^v)$. In what follows, we first show that the feasible space $\mathcal{M}$ is compact and convex, then demonstrate a continuous mapping from $(\mathbf{m}^c, \mathbf{m}^v)$ to themselves.

Lemma 3. *$\mathcal{M}$ is compact and convex.*

Proof. First, we demonstrate that $\mathcal{M}$ is compact. Since $(\mathbf{m}^c, \mathbf{m}^v)$ are average numbers of awaiting bundles/drivers and demand flow, they are continuous variables, and thus the feasible space $(\mathbf{m}^c, \mathbf{m}^v)$ is closed in its interior. Since the total number of delivery drivers should be no more than the fleet size, the non-negative number $\mathbf{m}^v$ is bounded by its definition. Also, according to our assumption that the number of vacant drivers is more than the number of order bundles, the non-negative number $\mathbf{m}^c$ is also bounded. Then we have $0 \leq \mathbf{m}^c \leq \hat{\mathbf{m}}^c$ and $0 \leq \mathbf{m}^v \leq \hat{\mathbf{m}}^v$, where $\hat{\mathbf{m}}^c$ and $\hat{\mathbf{m}}^v$ denote the upper bounds for $\mathbf{m}^c$ and $\mathbf{m}^v$, respectively. Therefore, $\mathcal{M}$ is bounded and closed then thus compact, and it is also convex because its domain is a polyhedron. ■

Lemma 4. *The vacant driver flow and the customers' demand rate are functions of $\mathbf{m}^c$ and $\mathbf{m}^v$.*

Proof. According to Equation (5), the utility of vacant drivers is related to $\mathbf{m}^v$ by definition. Vacant drivers' utility is also related to the matching rate which is impacted by $\mathbf{m}^c$. Therefore, the vacant driver flow is a function of $\mathbf{m}^c$ and $\mathbf{m}^v$. According to Equation (2), the customers' utility is a

function of $\mathbf{m}^c$ by definition, and also a function of the matching rate which is impacted by $\mathbf{m}^v$. Therefore, the customers' demand rate is a function of $\mathbf{m}^c$ and $\mathbf{m}^v$. ■

Lemma 5. *$\mathbf{m}^c$ and $\mathbf{m}^v$ are functions of the vacant driver flow and the customers' demand rate.*

Proof. From Equation (1) we know that $\mathbf{m}^c$ and $\mathbf{m}^v$ are solved by the equilibrium conditions, where the equilibrium conditions include food delivery demand–supply and the flow conservation conditions. Therefore, $\mathbf{m}^c$ and $\mathbf{m}^v$ are dependent on the vacant driver flow and the customers' demand rate which make $\mathbf{m}^c$ and $\mathbf{m}^v$ functions of $\boldsymbol{\lambda}^{\varphi}$ and $\mathbf{q}$. ■

With Lemmas 4 and 5, we can establish a continuous mapping from $\mathbf{m}^c$ and $\mathbf{m}^v$ to themselves, i.e., $(\mathbf{m}^c, \mathbf{m}^v) = \Gamma_1(\boldsymbol{\lambda}^{\varphi}, \mathbf{q}) = \Gamma_1(\Gamma_2(\mathbf{m}^c, \mathbf{m}^v)) = \Gamma(\mathbf{m}^c, \mathbf{m}^v)$. Then, the second condition of Brouwer's fixed-point theorem is satisfied, and this completes the proof of the existence of the equilibrium.

Appendix G Flow of each delivery path

Table 6: Flow of paths under DCS

	Merchant	Slot 1	Slot 2	Slot 3	Slot 4	Flow
0	1	1	1	1	1	13.707
1	1	2	2	2	2	5.4402
2	1	2	3	3	3	0.4015
3	1	5	5	5	4	2.4059
4	1	4	6	6	6	0.0117
5	1	5	5	5	5	7.3406
6	1	7	7	7	7	4.9357
7	1	8	8	8	8	0.0006
8	2	1	1	1	1	7.9270
9	2	2	2	2	2	58.121
10	2	3	3	3	3	7.4975
11	2	5	5	5	4	0.7410
12	2	5	4	6	6	0.0056
13	2	5	5	5	5	9.8212
14	2	7	7	7	7	6.1088
15	2	8	8	8	8	0.0033
16	3	2	1	1	1	0.4474
17	3	2	2	2	2	5.4956
18	3	2	5	5	5	0.5855

Page over

Table 6: Flow of paths under DCS continued

Path index	Merchant	Slot 1	Slot 2	Slot 3	Slot 4	Flow
19	3	3	3	3	3	17.246
20	3	7	7	7	7	1.8119
21	3	8	8	8	8	0.0123
22	4	1	1	1	1	2.5442
23	4	1	7	7	7	0.3951
24	4	5	2	2	2	0.7390
25	4	4	4	4	4	5.5580
26	4	5	5	5	5	10.993
27	4	6	6	6	6	0.1535
28	5	4	/	/	/	38.996
29	5	1	1	1	1	10.075
30	5	1	7	7	7	1.5791
31	5	2	2	2	2	8.2086
32	5	2	3	3	3	0.6022
33	5	4	6	6	6	0.0811
34	5	5	5	5	5	35.105
35	6	4	1	1	1	0.0188
36	6	4	5	2	2	0.0060
37	6	4	4	4	4	0.1713
38	6	4	5	5	5	0.1097
39	6	6	6	6	6	0.2251
40	7	1	1	1	1	3.6179
41	7	1	5	5	4	0.2368
42	7	1	5	5	5	0.9415
43	7	2	2	2	2	3.4765
44	7	3	3	3	3	1.3234
45	7	7	7	7	7	15.344
46	7	8	8	8	8	0.0032
47	8	7	1	1	1	0.0036
48	8	3	2	2	2	0.0133
49	8	3	3	3	3	0.0484
50	8	7	7	7	7	0.0176
51	8	8	8	8	8	0.2754

Table 7: Flow of paths under WTS

	Merchant	Slot 1	Slot 2	Slot 3	Slot 4	Flow
0	1	3	/	/	/	0.5741
1	1	4	/	/	/	6.5072
2	1	6	/	/	/	0.0133
3	1	8	/	/	/	0.0006
4	1	1	1	/	/	26.051
5	1	2	2	/	/	9.5368
6	1	5	5	/	/	16.511
7	1	7	7	/	/	8.8777
8	2	4	/	/	/	1.5285
9	2	6	/	/	/	0.0049
10	2	8	/	/	/	0.0037
11	2	1	1	1	/	10.432
12	2	2	2	2	/	77.614
13	2	3	3	3	/	9.8296
14	2	5	5	5	/	13.558
15	2	7	7	7	/	8.1205
16	3	1	/	/	/	0.6796
17	3	3	/	/	/	65.311
18	3	5	/	/	/	0.8646
19	3	7	/	/	/	4.5048
20	3	8	/	/	/	0.0196
21	3	2	2	/	/	10.184
22	4	1	/	/	/	5.8778
23	4	2	/	/	/	0.8910
24	4	4	/	/	/	14.593
25	4	6	/	/	/	0.2913
26	4	7	/	/	/	0.4739
27	4	5	5	/	/	17.106
28	5	3	/	/	/	0.8286
29	5	6	/	/	/	0.1181
30	5	7	/	/	/	2.5534
31	5	4	4	/	/	20.922
32	5	1	1	1	/	13.658
33	5	2	2	2	/	10.533

Page over

Table 7: Flow of paths under WTS continued

Path index	Merchant	Slot 1	Slot 2	Slot 3	Slot 4	Flow
34	5	5	5	5	5	34.845
35	6	1	/	/	/	0.0197
36	6	2	/	/	/	0.0046
37	6	4	/	/	/	0.4777
38	6	5	/	/	/	0.1542
39	6	6	/	/	/	0.6668
40	7	3	/	/	/	3.0594
41	7	4	/	/	/	0.4218
42	7	5	/	/	/	1.8095
43	7	7	/	/	/	56.254
44	7	8	/	/	/	0.0039
45	7	1	1	/	/	6.8668
46	7	2	2	/	/	5.6420
47	8	1	/	/	/	0.0028
48	8	2	/	/	/	0.0119
49	8	3	/	/	/	0.0833
50	8	7	/	/	/	0.0243
51	8	8	/	/	/	0.9141

Appendix H The flow of drivers in networks

Figure 15 presents the origin-destination (OD) flow for pickup and vacant drivers and the origin-throughput (OT) flow for occupied drivers under three dispatching strategies. Note that the OT flow is equal to the customer demand, so it also represents the customer demand rate in the network.

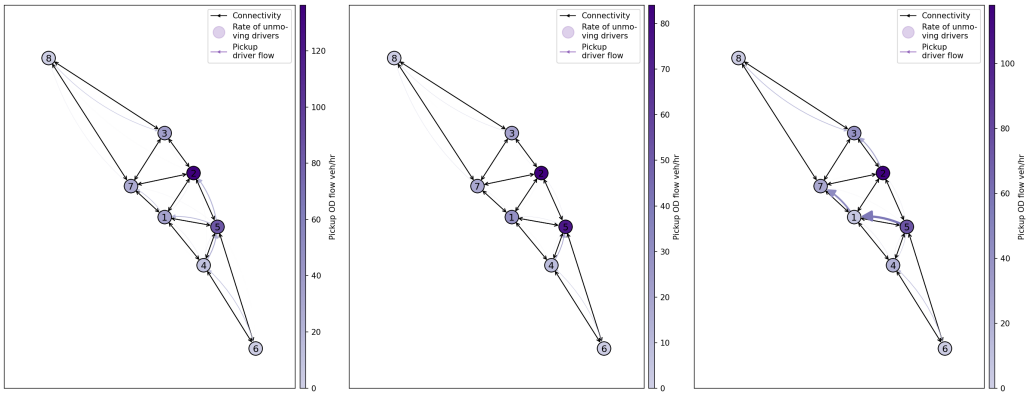

(a) Matching OD flow, RBS **(b)** Matching OD flow, DCS **(c)** Matching OD flow, WTS

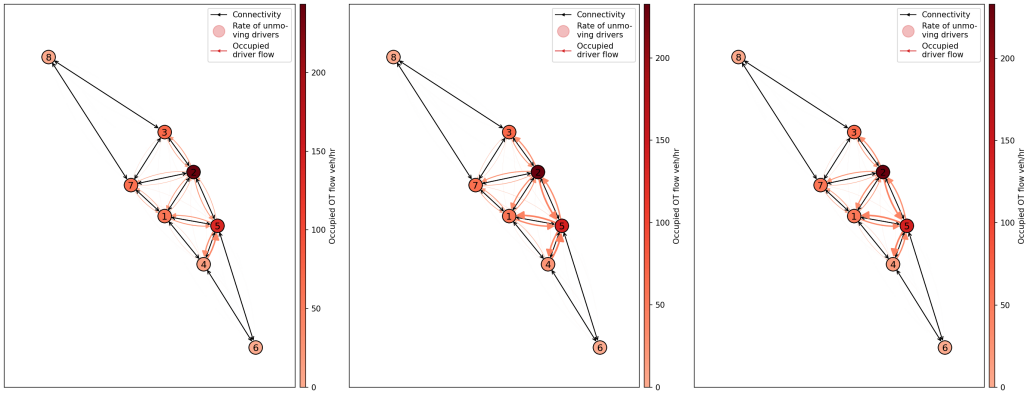

(d) Occupied OT flow, RBS **(e)** Occupied OT flow, DCS **(f)** Occupied OT flow, WTS

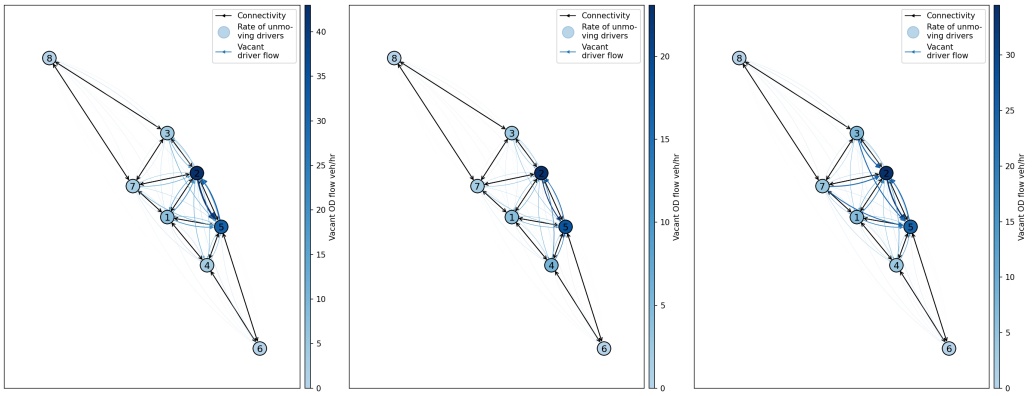

(g) Vacant OD flow, RBS **(h)** Vacant OD flow, DCS **(i)** Vacant OD flow, WTS

Figure 15: The network with 8 regions.

Appendix I Extension to a more complex network

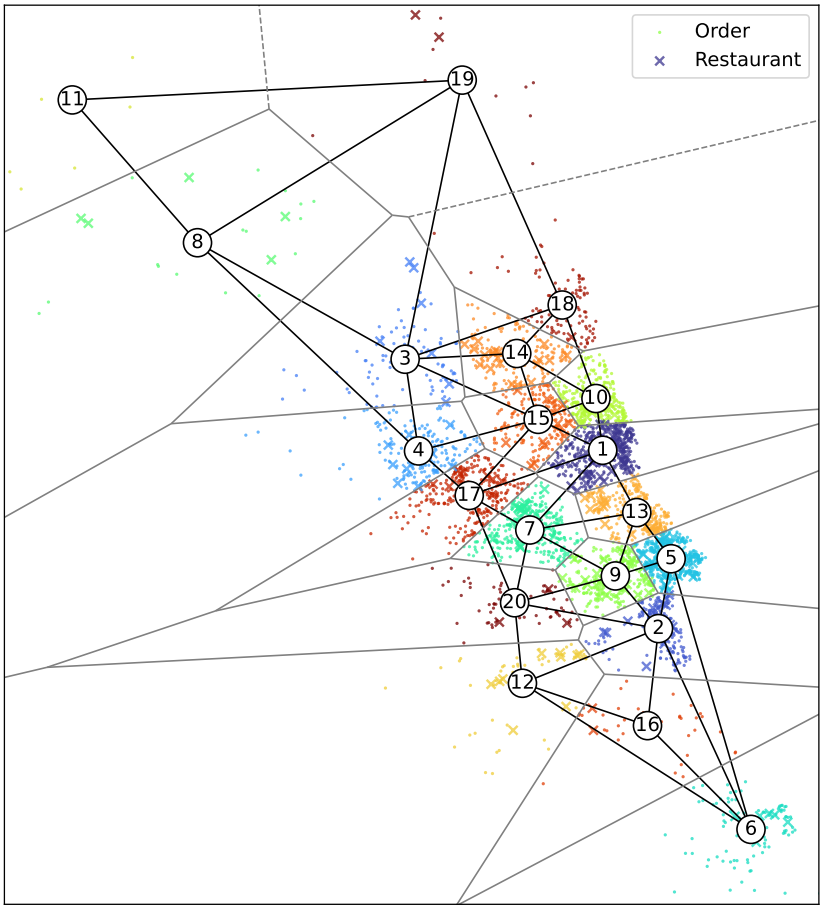

Figure 16: The region partition to 20 regions

Figure 16 shows our partitioning of the studied region into 20 regions. As mentioned earlier, the number of decision variables has increased to 27024 for the delivery path flow, 400 for the matching flow, and 460 for unknown variables ($\mathbf{q}$ and $\mathbf{m}$).

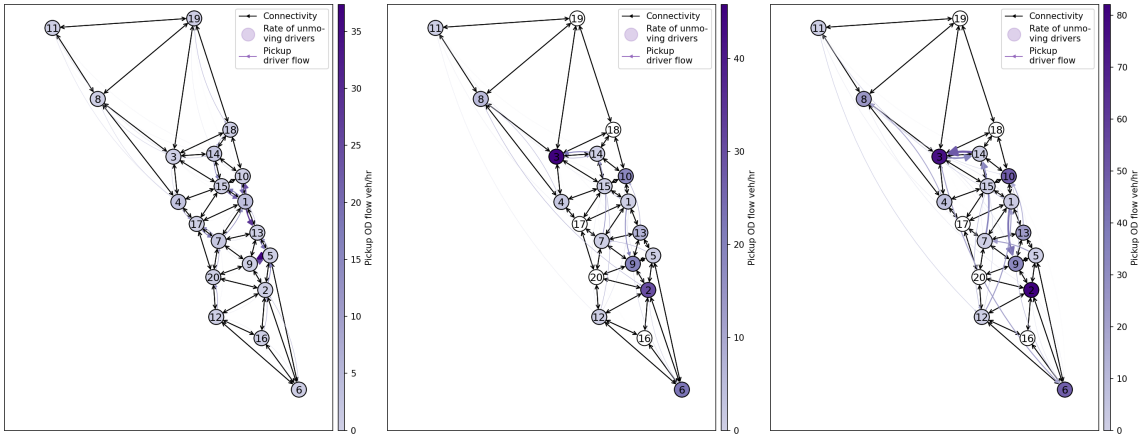

(a) Matching OD flow, RBS **(b)** Matching OD flow, DCS **(c)** Matching OD flow, WTS

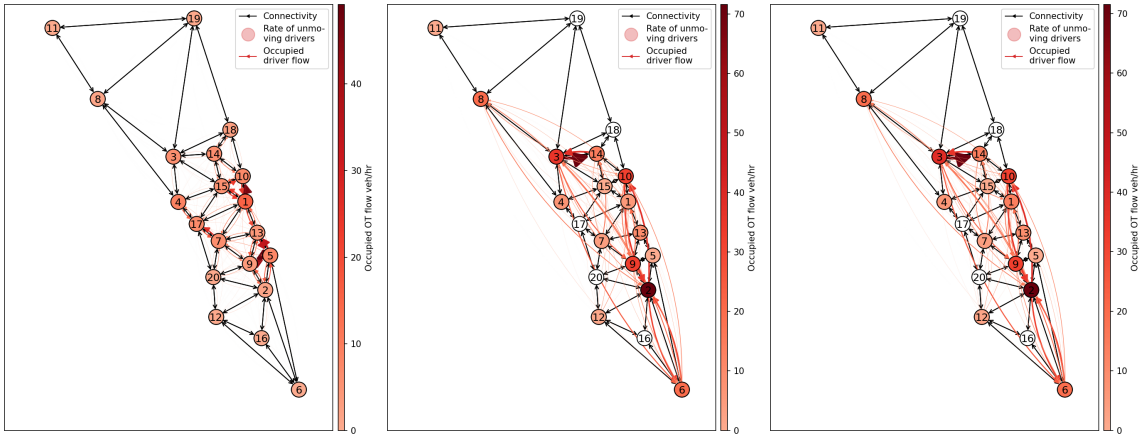

(d) Occupied OT flow, RBS **(e)** Occupied OT flow, DCS **(f)** Occupied OT flow, WTS

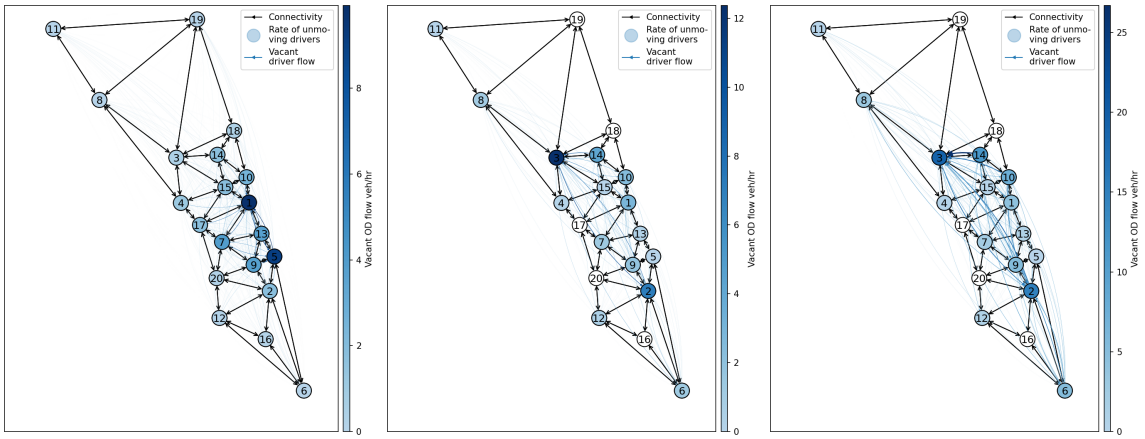

(g) Vacant OD flow, RBS **(h)** Vacant OD flow, DCS **(i)** Vacant OD flow, WTS

Figure 17: The network with 20 regions